Preprint; cite as *Langmuir*, 2016, **32** *(35)*, pp 8858–8871

Adsorption of ions at uncharged insoluble monolayers

Tatyana V. Peshkova,[†] Ivan L. Minkov,[‡,†] Roumen Tsekov,[†] Radomir I. Slavchov*[,†,§]

[†]*Department of Physical Chemistry, Faculty of Chemistry and Pharmacy, Sofia University, 1 J. Bourchier Blvd., 1164 Sofia, Bulgaria*
[‡]*Department of Chemistry, Biochemistry, Physiology, and Pathophysiology, Faculty of Medicine, Sofia University, 1 Koziak Str., 1407 Sofia, Bulgaria*
[§]*Department of Chemical Engineering and Biotechnology, Cambridge University, Pembroke Street, New Museums Site, CB2 3RA Cambridge, United Kingdom*
**E-mail: ris26@cam.ac.uk*

KEYWORDS: adsorption of ions, Langmuir monolayer, uncharged monolayer, Hofmeister series, concentrated electrolyte, equilibrium spreading pressure

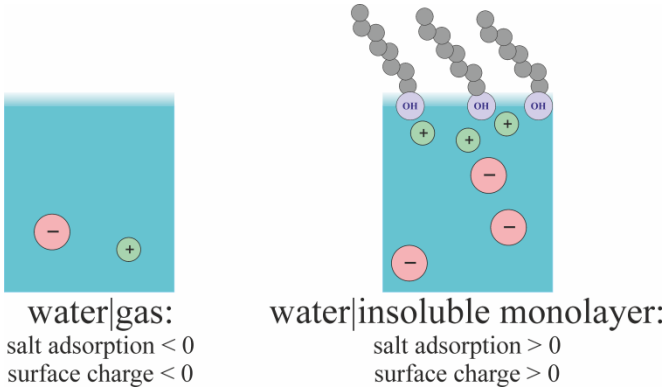

ABSTRACT: A method is proposed for the experimental determination of the adsorption of inorganic electrolytes at a surface covered with insoluble surfactant monolayer. This task is complicated by the fact that the change of the salt concentration alters both chemical potentials of the electrolyte and the surfactant. Our method resolves the question by combining data for the surface pressure vs. area of the monolayer at several salt concentrations with data for the equilibrium spreading pressure of crystals of the surfactant (used to fix a standard state). We applied the method to alcohols spread at the surface of concentrated halide solutions. The measured salt adsorption is positive and has non-monotonic dependence on the area per surfactant molecule. For the liquid expanded film, depending on the concentration, there is one couple of ions adsorbed per each 3-30 surfactant molecules. We analyzed which ion, the positive or the negative, stands closer to the surface, by measuring the effect of NaCl on the Volta potential of the monolayer. The potentiometric data suggest that Na^+ is specifically adsorbed, while Cl^- remains in the diffuse layer, i.e. the surface is positively charged. The observed reverse Hofmeister series of the adsorptions of NaF, NaCl and NaBr suggests the same conclusion holds for all these salts. The force that causes the adsorption of Na^+ seems to be the interaction of the ion with the dipole moment of the monolayer.

INTRODUCTION

When NaCl is added to water, the surface tension σ of the solution increases[1]. According to the Gibbs isotherm, this means that NaCl has negative adsorption at the surface of the aqueous solution, i.e. its concentration near the surface is diminished compared to the bulk[2]. This is only possible if the ions are repelled from the surface. This repulsion is insensitive to the nature of the hydrophobic phase. If NaCl is added to water in contact with *oil*, the interfacial tension increment at the water|non-polar oil interface (W|O) follows a dependence on the concentration C_m that matches almost exactly[1,3] $\sigma(C_m)$ at water|gas (W|G; Figure S1).

The nature of the repulsive forces that act on Na^+ and Cl^- seems to be well understood: these are the screened image potential at low concentration[4] and the hydration repulsion at high[5]. The same two forces – image and hydration – allow for the quantitative understanding of the surface tension[6], the interfacial tension[7] and the surface dipolar χ-potential[8] of a NaCl solution. The model holds with good accuracy for many salts (any combination of Li^+, Na^+, K^+, Rb^+, Cs^+, Mg^{2+}, Ca^{2+}, Ba^{2+}, La^{3+}, OH^-, F^-, Cl^-, SO_4^{2-}, CO_2^{2-}), provided that the bulk activity coefficients and the surface charge accumulated due to the difference in the ion hydration are accounted for[7,6,8].

The picture is different for salts containing large anions. If one adds NaBr or NaI to water, the surface tension again increases[1,9]; however, compared to NaCl, the increase for NaI is weaker (Figure S1). This means that I^- are repelled by the water surface to a lesser extent than Cl^-. The surface χ-potential of solutions of NaBr and NaI also cannot be explained with image and hydration forces only – the values of $\Delta\chi$ suggest that Br^- and I^- stand closer to the surface than the cation[8]. This is observed also in molecular dynamic simulations[10], X-ray photoelectron spectroscopy of the saturated solution[11] and vibrational sum frequency generation spectroscopy[12] (for NaBr – only above 1M). At the same time, no signs for surface enrichment with F^-, Cl^- or (at lower concentrations) Br^- were found by Liu et al.[12]. The X-ray reflectivity experiments[13] showed surface enrichment of the *cation* for NaCl & NaBr.

Unlike Na^+ and Cl^-, the interaction of the large anions with the interface depends on the hydrophobic phase. If the aqueous NaBr or NaI are in contact with an oil phase[6,14], the interfacial tension increment is rather different from the surface tension increment. In fact, the increase of the surface tension in the presence of NaBr is twice as high as the increase of the interfacial tension (Figure S1). The contrast is even stronger with NaI – this salt weakly increases the surface tension, and *decreases* the interfacial tension, i.e. NaI is adsorbed at W|O.

The nature of the attractive force which pulls Br^- and I^- to the interface is disputed in the literature. Some authors explain it with *attractive van der Waals* interaction[15,16]; others show that the *van der Waals force is actually repulsive* at the W|G[17] and almost absent at the W|O[18]; a third opinion is that van der Waals force is attractive at W|O and absent at the W|G[19]. Levin[20] developed a model which blamed the *hydrophobic* force for the attraction, see also ref [21]. The qualitative comparison of the tensiometric data for W|G and W|O[7] leads to the conclusion that the only combination of van der Waals and hydrophobic interactions that does not contradict the experimental data is the following: **(i)** ions at the W|G are subject to repulsive van der Waals and attractive hydrophobic force, which compensate each other almost completely, and **(ii)** the substitution of the air with an oil phase switches off the repulsive dispersion interaction while the hydrophobic attraction remains unchanged. However, the ions might be subject to numerous other specific forces – e.g., ion-surface dipole interactions[22] – which have not been studied in detail. Therefore, the question remains open.

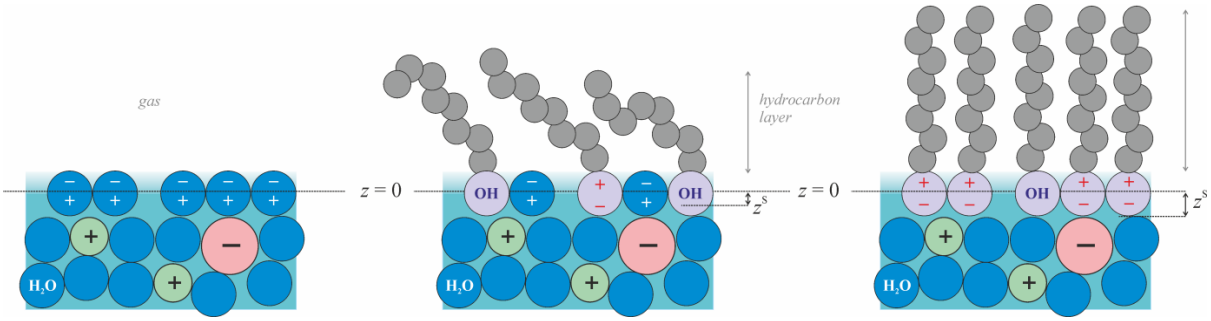

Figure 1. Schematic illustration of the effect of the surfactant on the structure of the aqueous surface. The hydroxyl groups penetrate in the polar phase ($z < 0$), leading to a shift z^S of the Gibbs equimolecular surface with respect to the surface of discontinuity of the dielectric permittivity ($z = 0$). They also change the sign of the surface dipole from negative to positive toward air, passing through a point of zero dipole at a certain area $1/\Gamma_{P=0}$. With the decrease of the area per surfactant molecule, the thickness of the hydrophobic layer increases.

The promising results from the comparison between interfaces of varying hydrophobic phases lead us to the idea to investigate the interactions of ions and uncharged monolayers7. It is well-known that many surfactants form an oil-like *liquid expanded* (LE) film at the W|G surface[23,24]. By changing the area of the spread monolayer, one alters the thickness and the density of this LE film (Figure 1). When the LE film is thinner, the ion will interact with the surface as if it is W|G, and when it is thicker, the interaction should resemble ion-W|O interface. Hence, the main motivation of our work is to *investigate the ion-surface interaction and the Hofmeister effect in the presence of uncharged surfactant monolayers with variable density*.

The published data for the interaction between ions and surfactant monolayers already show that a picture involving only the set of forces discussed above is oversimplified. The same small ions that are repelled by both W|G and W|O may actually be attracted by the monolayer. One proof is the finding of Ralston and Healy[25] that the adsorption of KCl is very close to zero at the monolayer spread around octadecanol crystals, while one would expect it to be closer to the negative value of the adsorption found for KCl at the water|decanol interface[26] – i.e. there is a significant attraction of K^+ and Cl^- toward the condensed octadecanol monolayer that is absent at the neat W|G, W|alkane and W|decanol interfaces. The equilibrium spreading pressures of Frumkin and Pankratov[22] suggest that even salts that desorb8,7 strongly at W|G and W|O (K_2SO_4, $CaCl_2$) are actually adsorbed by the ethylpalmitate monolayer. Another indication for attraction is the effect of the electrolyte on the adsorption constant K_a of oil-soluble alcohols adsorbed at the oil|brine interface7 – the fact that the experimental values of K_a in *figure 5* in ref [7] stand above the theoretical line (that accounts for image and hydration forces only) points at additional ion-monolayer attraction.

However, the literature data for the *adsorption* Γ_{el} *of electrolytes* at a surface with a monolayer is scarce, and apart from the very fact that ion-monolayer attraction exists, little can be said about it. Its nature, magnitude, dependence on the monolayer density and C_m are still unrevealed. The tensiometric studies of *soluble* monolayers at the surface of salt solutions[26-28] do not allow Γ_{el} to be determined directly because of the salting-out effect (the electrolyte alters the bulk chemical potential of the surfactant making it impossible to change C_m at fixed chemical potential of the surfactant, as required by the Gibbs adsorption equation). An elegant experimental solution of this problem was given by Aveyard et al., who investigated a monolayer at the water|oil interface with electrolyte dissolved in the water and surfactant dissolved in the oil[26]; we considered these data previously7. The effect of the salt on the state of *insoluble* monolayers has been studied since the fathers of modern surface science[29-31,22], to newer works on uncharged[32,33] and charged[34,35] monolayers. It is remarkable that none of these studies could determine the most straightforward characteristic of the ion-monolayer interaction – the salt adsorption Γ_{el}. The reason is that it is principally impossible to find Γ_{el} based solely

on data for the surface pressure vs. area isotherms[22,25,7]. Therefore, the second purpose of our work is to *develop an experimental method for determination of the salt adsorption at a surface with spread insoluble monolayer*.

The third, more remote motivation of ours is that the method for measurement of Γ_{el} at a monolayer we propose below is providing a tool for quantitative investigation of the interaction between biologically relevant ions and the polar head groups of lipids and proteins. These interactions are involved[36] in the processes of membrane fusion, secretion and many others. The salt effect on the state of lipid monolayers was reviewed recently by Leontidis[21]. Short-ranged interactions between the ions and the polar head groups of the lipid were found to be significant with dipalmitoylphosphatidylcholine (DPPC) monolayers[37] and membranes[38]. In this work, the ion-polar head group interactions will be mentioned only briefly; we will discuss data for alcohols only, chosen because the interaction of the ions with the alcohol group is very similar to the interaction ion-water7, which simplifies the interpretation of the results. We will present a separate, detailed study of ions interacting with monolayers containing other head groups in a companion paper.

THEORETICAL BASIS

We first present the approach we developed for the determination of the electrolyte adsorption at an uncharged monolayer, based on the ideas of Frumkin and Pankratov[22]. Each step of our method will be immediately demonstrated on the example of the data by Ralston and Healy[25] for octadecanol monolayers spread on concentrated KCl solutions. These data are shown in Figure 2, in coordinates surface tension σ vs. area Γ^{-1} per surfactant molecule (which are more convenient for our purposes than the original surface pressure vs. area coordinates).

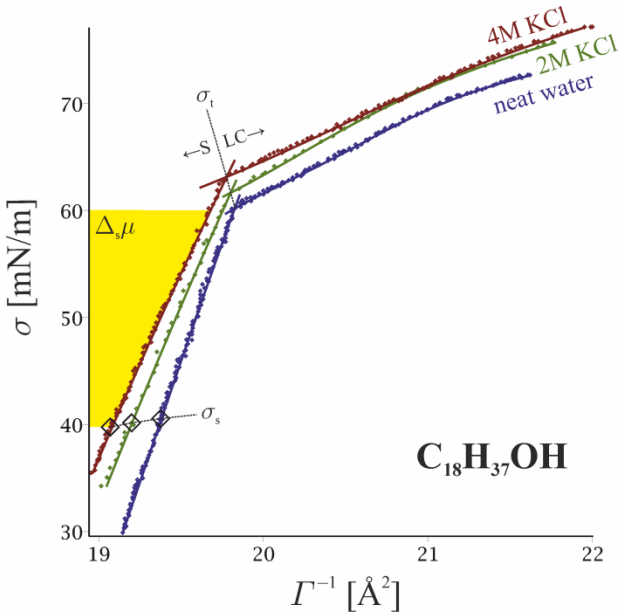

Figure 2. Surface tension σ vs. area per molecule Γ^{-1} for $C_{18}H_{37}OH$ monolayers spread on substrates of various concentrations of KCl. Points are data by Ralston and Healy[25]. Diamonds correspond to the equilibrium spreading tension σ_s of pure octadecanol crystals (chosen by us as standard state). Lines are polynomial fits of the inverse dependence $\Gamma^{-1}(\sigma)$ with eq (9). A 2nd order phase transition is evident at σ_t; we refer to the two phases as to *solid* (S) and *liquid condensed* (LC). The shaded area gives the chemical potential $\Delta_s\mu$ of the surfactant, eq (7).

The general thermodynamics of a monolayer spread on electrolyte solution has been investigated previously[22,25,7]. The Gibbs isotherm of the monolayer in the presence of 1:1 electrolyte in the substrate reads:

$$\mathrm{d}\sigma = -2\Gamma_{\mathrm{el}}\mathrm{d}\mu_{\mathrm{el}} - \Gamma\mathrm{d}\mu\,, \tag{1}$$

where Γ and Γ_{el} are the Gibbs adsorptions of the surfactant and the electrolyte at water's equimolecular surface[6,39]; the electrolyte adsorption is multiplied by van 't Hoff's isotonic coefficient 2. The chemical potentials of the surfactant and the electrolyte are related to Γ and C_{m} as

$$\mu = \mu_0^{\mathrm{S}} + T\ln\gamma^{\mathrm{S}}\Gamma \quad \text{and} \quad \mu_{\mathrm{el}} = \mu_{\mathrm{el0}} + T\ln\gamma_{\pm}C_{\mathrm{m}}\,, \tag{2}$$

where T is the thermodynamic temperature (T[J] = $k_{\mathrm{B}}T$[K]), μ_0 are standard chemical potentials, γ^{S} is the surface activity coefficient of the surfactant, $\gamma_{\pm}$ is the bulk mean activity coefficient of the electrolyte (a list of symbols is given in S1).

Expressing from eq (1) the derivative of σ with respect to μ_{el} at constant Γ, and isolating Γ_{el} from the resulting relation, one obtains:

$$\Gamma_{\mathrm{el}} = -\frac{1}{2}\left(\frac{\partial\sigma}{\partial\mu_{\mathrm{el}}}\right)_{\Gamma} - \frac{\Gamma}{2}\left(\frac{\partial\mu}{\partial\mu_{\mathrm{el}}}\right)_{\Gamma}. \tag{3}$$

Ralston and Healy[25] neglected the last term in this equation and estimated Γ_{el} as $-\frac{1}{2}(\partial\sigma/\partial\mu_{\mathrm{el}})_{\Gamma}$, to which we refer as to *Ralston-Healy approximation*. For the data in Figure 2, the surface tension at fixed Γ increases with the increase of C_{m}, which means that, in the Ralston-Healy approximation, the adsorption of KCl at the octadecanol monolayer is negative ($\Gamma_{\mathrm{el}} < 0$). However, this approximation is rough[25]. To demonstrate that, we substitute eqs (2) in eq (3):

$$\Gamma_{\mathrm{el}} = -\frac{\gamma_{\pm}C_{\mathrm{m}}}{2T}\left(\frac{\partial\sigma}{\partial\gamma_{\pm}C_{\mathrm{m}}}\right)_{\Gamma} - \frac{\gamma_{\pm}C_{\mathrm{m}}\Gamma}{2T}\left(\frac{\partial\mu_0^{\mathrm{S}}}{\partial\gamma_{\pm}C_{\mathrm{m}}}\right)_{\Gamma} - \frac{\gamma_{\pm}C_{\mathrm{m}}\Gamma}{2}\left(\frac{\partial\ln\gamma^{\mathrm{S}}}{\partial\gamma_{\pm}C_{\mathrm{m}}}\right)_{\Gamma}. \tag{4}$$

The first term here is Γ_{el} in the Ralston-Healy approximation. It can be calculated from the data in Figure 2, and is of the order of 0.1 nm^{-2}. The second term reflects the direct interaction between the ions and a *single* adsorbed surfactant molecule. We can deal with it using the approximate dependence on C_{m} of the standard chemical potential μ_0^{S} of the alcohol in the monolayer derived in ref [7]:

$$\mu_0^{\mathrm{S}}(C_{\mathrm{m}}) = \mu_0^{\mathrm{S}}(0) - 2TM_{\mathrm{w}}\gamma_{\mathrm{w}}C_{\mathrm{m}}\,; \tag{5}$$

here M_{w} is the molar mass of water, γ_{w} is the osmotic coefficient of the solution and $\mu_0^{\mathrm{S}}(0)$ is monolayer's standard potential in the absence of electrolyte. Eq (5) is valid for alcohols and for small ions only; its validity was proven for ionic strengths in the range 0-1M, but it is inexact at higher concentrations[7]. Eq (5) can be considered as a theory of the surface Setschenow coefficient of an alcohol monolayer (a quantity similar to the micellar Setschenow constant[40]). Using eq (5) together with the Gibbs-Duhem relation $\mathrm{d}(\gamma_{\mathrm{w}}C_{\mathrm{m}}) = C_{\mathrm{m}}\mathrm{d}\ln\gamma_{\pm}C_{\mathrm{m}}$, one finds that the second term in eq (4) is equal to $M_{\mathrm{w}}C_{\mathrm{m}}\Gamma$, which is of the order of 0.1 nm^{-2} for the data in Figure 2. Thus, the first two terms in eq (4) are of similar magnitude. The third term in eq (4) stands for the effect of the electrolyte in the substrate on the lateral interaction between the surfactant molecules in the monolayer, and is significant as well[7,22]. Hence, none of the three contributions in eq (4) is negligible.

Let us show now how the results in Figure 2 combined with the data of Ralston and Healy[25] for the equilibrium spreading tension of octadecanol crystals allow for the precise determination of Γ_{el}. From eq (1), the Gibbs-Duhem relation for the surface follows:

$$2\Gamma_{\mathrm{el}} = -\Gamma\left(\frac{\partial\mu}{\partial\mu_{\mathrm{el}}}\right)_{\sigma}. \tag{6}$$

To use this equation, one needs the dependence of surfactant's chemical potential μ on C_m and σ. The potential μ can be obtained by integration[22] of the Gibbs isotherm (1) at fixed electrolyte concentration ($d\mu = -\Gamma^{-1}d\sigma$) starting from certain suitably chosen *standard state* (subscript "s"):

$$\Delta_s\mu \equiv \mu - \mu_s = -\int_{\sigma_s}^{\sigma} \Gamma^{-1}d\sigma . \qquad (7)$$

The integral can be calculated numerically from the experimental σ vs. Γ data (e.g., the area of the shaded area in Figure 2 continued to $\Gamma^{-1} = 0$ is equal to the value of $\Delta_s\mu$ at 60 mN/m and 4M KCl). Provided that the chemical potential μ_s of the standard state is *independent on the electrolyte concentration*, one can substitute μ in the Gibbs-Duhem eq (6) with $\Delta_s\mu = \mu - \mu_s$:

$$2\Gamma_{el} = -\Gamma\left(\frac{\partial\Delta_s\mu}{\partial\mu_{el}}\right)_\sigma = -\frac{\Gamma\gamma_\pm C_m}{T}\left(\frac{\partial\Delta_s\mu}{\partial\gamma_\pm C_m}\right)_\sigma . \qquad (8)$$

Thus, if one disposes of a function $\sigma_s(C_m)$ that corresponds to certain fixed, C_m-independent chemical potential μ_s of the monolayer, the calculation of the integral (7) and Γ_{el} through eq (8) is straightforward.

A very convenient standard state is the one corresponding to a monolayer spread around pure crystals of the surfactant floating at the surface of the brine[22]. Indeed, μ of this monolayer is fixed to the chemical potential of the crystal, which is independent of the concentration C_m of the electrolyte. The data for the surface tension $\sigma_s(C_m)$ of the monolayer spread around octadecanol crystals[25] are illustrated in Figure S3. The data show that σ_s is nearly constant, decreasing by less than 2 mN/m for 0-4M KCl. As for these data surfactant's potential μ_s is constant, from eq (1) it follows immediately[25] for the electrolyte concentration that $\Gamma_{el,s} = -½\partial\sigma_s/\partial\mu_{el}$; therefore, the small negative slope in Figure S3 corresponds to a small positive salt adsorption ($\Gamma_{el,s}$ = 0.037±0.02 and 0.083±0.04 nm^{-2} for 2 and 4M KCl respectively; the activity of KCl is from ref [41]). The spreading tensions are shown also in Figure 2 (diamonds); note that the data for the monolayer compressed to $\sigma < \sigma_s$ correspond to metastable monolayer[42] that would relax to octadecanol crystals dispersed in an equilibrium spread layer, were the nucleation process fast enough.

Using the σ_s and $\sigma(\Gamma^{-1})$ data in Figure 2, we can calculate $\Delta_s\mu$ through eq (7) at each experimental concentration. To perform the integration, we first interpolate the data. The application of eq (7) is easier if the inverse function, area per surfactant Γ^{-1} vs. surface tension σ, is used. A complication is the existence of a 2nd order phase transition from a less condensed phase (*liquid condensed*, superscript LC) to a more condensed one (*solid*[43], S). In such case, a stepwise regression function with discontinuous 1st derivative is appropriate – we used the following polynomial:

$$\Gamma^{-1}(\sigma) = \begin{cases} \Gamma_t^{-1} + g_1^{LC}(\sigma-\sigma_t) + ... + g_4^{LC}(\sigma-\sigma_t)^4, & \sigma > \sigma_t; \\ \Gamma_t^{-1} + g_1^{S}(\sigma-\sigma_t) + ... + g_4^{S}(\sigma-\sigma_t)^4, & \sigma < \sigma_t. \end{cases} \qquad (9)$$

Here, Γ_t and σ_t are setting the point of the phase transition and are considered parameters of the regression function, along with the g-coefficients (related to the compressibility of the monolayer). Usually, a parabola or a cubic polynomial would interpolate the data for each surface phase in Figure 2 well – in these cases, the coefficients $g_{3\text{-}4}$ were set to zero. The parameters are summarized in Table S2, and the three functions (9) are plotted together with the experimental data for the three salt concentrations in Figure 2 (lines).

The substitution of the regression function (9) in the integral (7) leads to an explicit dependence of the chemical potential of the surfactant on σ,

$$\Delta_s\mu = \begin{cases} \Delta_s\mu_t - \Gamma_t^{-1}(\sigma-\sigma_t) - g_1^{LC}(\sigma-\sigma_t)^2/2 - \ldots - g_4^{LC}(\sigma-\sigma_t)^5/5, & \sigma > \sigma_t; \\ \Delta_s\mu_t - \Gamma_t^{-1}(\sigma-\sigma_t) - g_1^{S}(\sigma-\sigma_t)^2/2 - \ldots - g_4^{S}(\sigma-\sigma_t)^5/5, & \sigma < \sigma_t. \end{cases} \quad (10)$$

Here, the parameter $\Delta_s\mu_t$ (which is the value of $\Delta_s\mu$ at the point of the phase transition) stands for

$$\Delta_s\mu_t = \Gamma_t^{-1}(\sigma_s-\sigma_t) + g_1^{S}(\sigma_s-\sigma_t)^2/2 + \ldots + g_4^{S}(\sigma_s-\sigma_t)^5/5. \quad (11)$$

The chemical potential (10) is illustrated in Figure S4, in coordinates σ vs. $\Delta_s\mu$. The tensiometric data represented in these coordinates allow the sign of Γ_{el} to be determined immediately without assumptions. At fixed $\Delta_s\mu$, the surface tension *decreases* (although weakly) with the increase of the electrolyte concentration, which, according to the Gibbs equation (1), means that the electrolyte adsorption is positive (contrary to what follows from Ralston-Healy approximation $\Gamma_{el} \approx -\frac{1}{2}(\partial\sigma/\partial\mu_{el})_\Gamma$ and Figure 2, but in agreement with the positive $\Gamma_{el,s}$ of KCl at the monolayer spread around the octadecanol crystals).

Once $\Delta_s\mu(\sigma)$ is known at several concentrations of the electrolyte, one can calculate Γ_{el} through the Gibbs-Duhem relation (6) using the formulae for numerical differentiation (3 points central & backward finite difference):

$$\left(\frac{dy}{dx}\right)_2 = -\frac{x_3-x_2}{(x_3-x_1)(x_2-x_1)}y_1 + \frac{x_1-2x_2+x_3}{(x_3-x_2)(x_2-x_1)}y_2 + \frac{x_2-x_1}{(x_3-x_2)(x_3-x_1)}y_3, \quad (12)$$

$$\left(\frac{dy}{dx}\right)_3 = \frac{x_3-x_2}{(x_3-x_1)(x_2-x_1)}y_1 - \frac{x_3-x_1}{(x_3-x_2)(x_2-x_1)}y_2 + \frac{2x_3-x_1-x_2}{(x_3-x_2)(x_3-x_1)}y_3. \quad (13)$$

We use these formulae to represent the function $dy/dx = (\partial\Delta_s\mu/\partial\gamma_\pm C_m)_\sigma$ in eq (8) as a linear combination of the three functions $y_i = \Delta_s\mu(\sigma;\ \gamma_\pm C_{m,i})$, eq (10), at the three different concentrations $C_{m,1\text{-}3}$. The backward finite difference (13) is of much lower precision and we use it only for illustrative purposes. In most cases, we use the data for three concentrations to calculate the adsorption Γ_{el} corresponding to the central value only, with eq (12). Thus, using for $x_{1\text{-}3}$ the values[41] of the KCl activities ($\gamma_\pm C_m$ = 0, 1.22, and 2.69 mol/kg for 0, 2 and 4M respectively), and for $y_{1\text{-}3}$ – the three functions $\Delta_s\mu(\sigma)$ corresponding to these concentrations (eq (10) with the parameters from Table S2), from eq (12) we obtain the derivative $(\partial\Delta_s\mu/\partial\gamma_\pm C_m)_\sigma$ at 2M and from eq (13) – a less precise expression for $(\partial\Delta_s\mu/\partial\gamma_\pm C_m)_\sigma$ at 4M. Hence, the combination of eqs (8),(10),(12)&(13) give Γ_{el} as a function of σ. It is illustrated in Figure 3 (*left*).

We attempted to find the error of the so obtained electrolyte adsorption Γ_{el} by varying different parameters of the procedure. We found that the most critical factor is the inaccuracy of the values of σ_s. We therefore varied the values of σ_s within their uncertainty limits (as illustrated by the dashed lines in Figure S3) and analysed the respective variation in the obtained Γ_{el} curves. This method allowed us to estimate the uncertainty of Γ_{el}(2M KCl) at ±0.04 nm^{-2} (of the order of the absolute value of Γ_{el}) and of Γ_{el}(4M KCl) at ±0.15 nm^{-2} (twice the value of Γ_{el}). As Γ_{el} of KCl is close to zero, the results are not of high relative precision. The absolute precision (±0.04 nm^{-2}) is adequate, comparable with the standard tensiometric methods used for the determination of Γ_{el} of electrolytes at, e.g., water|gas. In view of the virtual absence of other methods for measurement of Γ_{el} at insoluble monolayers, the precision is satisfactory.

The numerical differentiation fails in the region between the values of the phase transition tension σ_t at the lowest and at the highest concentration (60.2–63.1 mN/m, cf. Table S2) – in this range of σ, one of the three $\Delta_s\mu$ values used for the calculation of the finite differences (12) &(13) is falling in a separate phase region than the other two, which means that the function that is differentiated is discontinuous. Therefore, between 60.2 and 63.1 mN/m, instead of

drawing the result from eqs (12)&(13), in Figure 3 we extrapolate manually the functions from the respective phase up to the phase transition point (dashed lines).

The results for Γ_{el} can be compared with the value of the adsorption $\Gamma_{el,s}$ at the equilibrium spreading tension following from the derivative of the line in Figure S3 – the results are marked with diamonds in Figure 3. The proximity of the lines and these points is a measure of the self-consistency of our procedure.

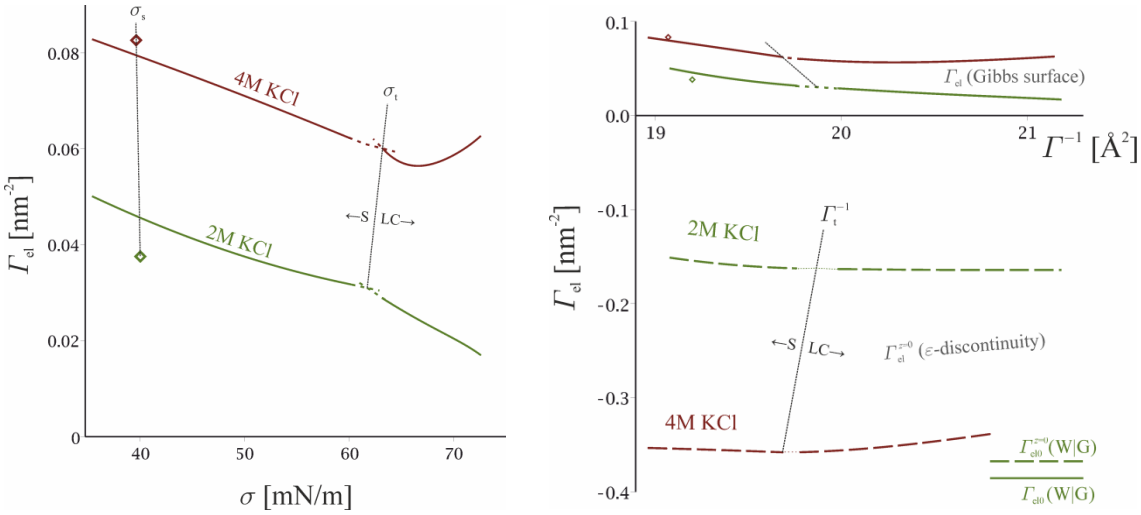

Figure 3. *Left:* the Gibbs adsorption Γ_{el} of KCl as a function of the surface tension of the octadecanol monolayer. Γ_{el} is calculated using eqs (8),(10),(12)&(13). *Right:* the Gibbs adsorption Γ_{el} and the adsorption of KCl at the ε-discontinuity surface, $\Gamma_{el}^{z=0}$, as functions of the area per surfactant molecule Γ^{-1} – a parametric plot of $\Gamma_{el}(\sigma)$ against $\Gamma^{-1}(\sigma)$. $\Gamma_{el}^{z=0}$ follows from eq (14).

The Gibbs adsorption Γ_{el} in eqs (3)&(4) corresponds to the Gibbs surface at which the adsorption of water is zero[44]. The position of this surface shifts in direction from the monolayer to the solution when the monolayer is compressed7 (Figure 1) and when electrolyte is added[39]. In order to make conclusions about the distribution of the ions with respect to the monolayer, it is more convenient to use the *surface of discontinuity of the dielectric permittivity and the density of the solution*7 (z = 0 superscript) that divides the hydrophilic from the hydrophobic phase. Its position was estimated7 to fall in the centre of mass of the last layer of water molecules and OH groups below the hydrocarbon layer (Figure 1), and remains there independently of Γ and C_m. The salt adsorptions Γ_{el} at the Gibbs and $\Gamma_{el}^{z=0}$ at the ε-discontinuity surface are related as follows7:

$$\Gamma_{el} = \frac{\Gamma_{el}^{z=0}}{1 - V_{el}C_M} + M_w C_m \Gamma ; \qquad (14)$$

here C_M is the molar concentration of the electrolyte. The term $M_w C_m \Gamma$ is due to the shift z^S of the Gibbs surface when surfactant's OH groups penetrate into the aqueous phase (Figure 1); it can also be understood as an osmotic effect due to the dilution of the water at the surface by the hydroxyl groups7 (the same effect is responsible for eq (5)). The denominator $1 - V_{el}C_M$ occurs in eq (14) due to the alteration of the profile of the water concentration resulting from the non-homogeneous distribution of the ions6,[39]. Eq (14) has been shown to be useful when the adsorption of small ions at water|alkane and water|fatty alcohol phase are compared – in this case, $\Gamma_{el}^{z=0}$(water|alkane) ≈ $\Gamma_{el}^{z=0}$(water|alcohol), i.e. the interaction of small ions with the surface of discontinuity of the dielectric permittivity is independent of the hydrophobic phase. At the same time, for the Gibbs adsorptions it is valid7 that Γ_{el}(water|alkane) < Γ_{el}(water|alcohol). Therefore, $\Gamma_{el}^{z=0}$ is a simpler measure of the ion-surface interaction than Γ_{el}.

The Gibbs and the ε-discontinuity adsorptions of the electrolyte, $\Gamma_{el}(\sigma)$ & $\Gamma_{el}^{z=0}(\sigma)$, are plotted in Figure 3 (*right*) against the area $\Gamma^{-1}(\sigma)$ per surfactant molecule, eq (9) (parametric plots with parameter σ). $\Gamma_{el}^{z=0}$ was calculated from Γ_{el} through eq (14). As seen in the figure, the two salt adsorptions are quite different, even of different sign. The K^+ and Cl^- ions are actually repelled by the surface of discontinuity of the dielectric permittivity, but due to the osmotic effect of the OH groups ($M_w C_m \Gamma$ in eq (14)), the Gibbs adsorption is still positive. Both Γ_{el} and $\Gamma_{el}^{z=0}$ are approximately proportional to the electrolyte concentration. In Figure 3 (*right*), the physical adsorption $\Gamma_{el}^{z=0}$ of KCl at 2M at the monolayer is compared also with the adsorption $\Gamma_{el\,0}^{z=0}$ of KCl at the neat W|G (cf. Table S1). Speaking of $\Gamma_{el}^{z=0}$, the neat surface desorbs twice as much KCl as the monolayer. From here the conclusion follows that there exists an attractive force pulling K^+ and Cl^- towards the monolayer that is absent at the neat W|G. Note that such attraction is absent at W|alkane or W|decanol7 as well, at least at concentrations below 1.5M KCl; therefore, this interaction it is either a feature of the concentrated solutions or of the monolayer structure.

Let us conclude this section with a brief discussion of the backward problem. Let us assume that the dependences $\Gamma_{el}(\Gamma, C_m)$ and $\sigma(\Gamma, C_m = 0)$ are known, and we want to find $\sigma(\Gamma, C_m)$ in the presence of salt. From the Gibbs isotherm (1), the following general solution of this problem is derived in S6:

$$\sigma(\Gamma, C_m) = \sigma(\Gamma, C_m = 0) + 2T\Gamma^2 \int_0^{C_m} \frac{\partial \Gamma_{el}(\Gamma, C_m)/\Gamma}{\partial \Gamma} \frac{\mathrm{d} \ln \gamma_{\pm} C_m}{\mathrm{d} C_m} \mathrm{d} C_m \,. \qquad (15)$$

From here it becomes clear why the knowledge of $\sigma(\Gamma, C_m)$ is insufficient to determine the salt adsorption $\Gamma_{el}(\Gamma, C_m)$: all functions $\Gamma_{el}(\Gamma, C_m)$ for which the derivative $\partial(\Gamma_{el}(\Gamma, C_m)/\Gamma)/\partial\Gamma$ is the same will lead to the same $\sigma(\Gamma, C_m)$. Therefore, measurements of $\sigma(\Gamma, C_m)$ allow the determination of $\Gamma_{el}(\Gamma, C_m)$ with accuracy up to an additive term $k(C_m)\Gamma$, where k is an arbitrary, C_m-dependant constant.

MATERIALS AND METHODS

Choice of surfactant. The main question in front of our study is the nature of the interaction between an ion and a *liquid* hydrophobic phase. We seek accordingly for the values of the salt adsorption at a monolayer in the LE state, which resembles liquid oil[23,24]. We chose to study alcohol monolayers because the interaction ion-water is similar to the one between an ion and a hydroxyl group, which simplifies the interpretation of the results7. At room temperature, only alcohols with $n \leq 12$ carbon atoms form LE films in a significant range of surface pressures (those with $n >$ 14-15 make a phase transition from gaseous directly to LC or solid phase, as in the case of the octadecanol in Figure 2). However, there is a problem with the shorter alcohols – those with $n <$ 12-13 have noticeable solubility. We chose to investigate dodecanol, since it is a reasonable compromise between solubility and stability of the LE phase. In addition, $C_{12}H_{25}OH$ monolayers have been studied previously with a variety of techniques[45-47], which allows us to validate our results against existing data. Some data for the equilibrium spreading tension of dodecanol and similar alcohols are also available[48,49,25].

Materials. All chemicals used by us were delivered by Sigma Aldrich: NaCl 99.8%, NaBr 99%, NaF 98.5%, and 1-dodecanol 98%. We also did experiments with NaI 99% and NaCl 99.999%, but the results were compromised by surface active impurities in these salt (a well-known problem with brines[50,51]). Water was double distilled with Elga Labwater, model PURELAB Option-Q7.

Measures against surface active impurities. We took various measures to control the adsorption of impurities at the investigated surfaces. First, we rinsed repeatedly the surface with the barrier before each run – a variant of a widely-used[51,52], simple and efficient procedure to clean the surface-active foulants. Second, before each compression of the monolayer, we did a control run – a compression without spread dodecanol. If decrease of the surface tension was detected, the surface was considered fouled. We finally did a set of tensiometric measurements with the surfaces that are carrying the highest risk of contamination – namely, neat W|G at the highest concentration of the salts. High C_m means higher concentration of impurities and higher surface activity of theirs (due to the salting-out effect), and neat surfaces are easier to contaminate than a surface with an existing dense monolayer (both for thermodynamic and kinetic reasons, cf. S2 & 4). This last test turned out to be very useful – it allowed us to check the efficiency of the rinsing of the surface against impurities, and with it we detected intolerable amounts of impurities in some of the salts we intended to use. We also tried baking the salts, but we found that rinsing is more efficient. Details are given in S2.

Methods. The monolayers were formed by spreading droplets from chloroform solutions of dodecanol (n_0 moles) uniformly over the available area (10.8×44 cm^2) of a Teflon trough on a sub-phase containing pure water or the investigated aqueous electrolyte. The spreading was performed with an Exmire micro syringe. The surface tension σ was measured using a KSV-2200 (Finland) surface balance equipped with a platinum plate. Measures needed to be taken to ensure complete wetting of the plate, see S2. With pure water and with 2 & 5 mol/kg NaCl, we measured simultaneously the surface ΔV potential with a gold-coated ^{241}Am ionizing electrode, a reference electrode and a KP 511 (Kriona, Bulgaria) electrometer, connected to a PC. As usual, the surface potential of the pure aqueous surface fluctuated for about 30 minutes. The reproducibility of the initial surface potential value was ±15 mV.

Once the surface W|G potential was stabilized, the monolayer was spread. Two kinetic experiments were performed: compression runs and isobaric runs. The *compression runs* are measurements of the surface tension σ and the surface ΔV potential as functions of *the apparent* area A/n_0 per surfactant molecule. After applying the chloroform droplets, a period of about 1 min was required for the evaporation of the solvent and the formation of a film. To obtain the isotherms, the films were compressed by means of shifting a barrier. Experiments with several different barrier velocities were performed (from 30 to 200 mm/min). At lower velocities, the monolayer had enough time to dissolve significantly and, in result, the whole σ vs. apparent area curve shifted toward smaller areas, cf. Figure S6 (*left*). The dissolution was less pronounced in the cases where the substrate was a concentrated electrolyte, due to the salting-out of the dodecanol (compare to the experiments of Lange and Jeschke[53], who used the salting-out to make their monolayers insoluble). We developed a procedure for the correction of the apparent area for the solubility of the monolayer, as described in S4. This procedure requires the independent measurement of the rate of dissolution of monolayers at fixed state (surface tension and *actual* adsorption that are constant with time). Therefore, we performed several *isobaric runs* for each compression run. The isobaric runs have an auxiliary function to our work, and their description is given in S4.

For large barrier velocities, the dissolution process is less important – for this reason, we performed most of our runs at 100 and 200 mm/min. This strategy has a drawback: due to the slow kinetics[54] of the LE-LC phase transition, the region of the phase transition shifts toward lower surface tensions, diverting from the theoretical horizontal line. The cause of this slow kinetics is probably the strong repulsion between the two-dimensional LC domains[55] (related to their pyroelectricity[56] – the domains carry macroscopic dipole moment normal to the surface), which stabilizes the two-dimensional dispersion of LC domains in the continuous LE phase. We corrected the data also for this effect, as explained in S4.

Equilibrium spreading tension σ_s of dodecanol. All salt solutions we used for these measurements were saturated with dodecanol for 12-24 hours in advance, at the required temperature. This was done to accelerate the experiment and to prevent the undesirable process of dissolution of the monolayer spread around the crystals. In theory, the saturated solution must have precisely the same equilibrium surface tension as σ_s of the crystals. However, the adsorption equilibrium is reached relatively slowly upon formation of a fresh surface – the spreading of the film around the dodecanol crystals leads to a much faster equilibration (through surface diffusion). We did some control tests with unsaturated substrates; in all cases, we found that, after the preliminary saturation with $C_{12}H_{25}OH$, the obtained values of σ_s are far more reproducible than those for spreading of crystals over the neat electrolyte.

The measurements were performed with a platinum plate and an analytic balance (Sartorius 211D) in a small Teflon trough equipped with two Teflon barriers. We used the two barriers to avoid the attachment of $C_{12}H_{25}OH$ crystals or drops to the meniscus of the plate (which affects the measured weight of the meniscus[25]), as described in S7. The initial value of the tension was usually higher, but is sometimes lower than σ_s, and on few occasions, it passed through an extremum. For each measurement, the surface tension was recorded for 5-10 min. It was found that the process of equilibration follows diffusion kinetics ($\sigma(t) - \sigma_s \propto const/t^{1/2}$, right from the start of the experiment or after a short initial period), probably due to a combination of two parallel processes: the rate determining surface diffusion (dodecanol spreads fast[49]) and a slower bulk diffusion (as the substrate is saturated with dodecanol in our setup). The data is accordingly extrapolated to $t \to \infty$, see S7.

RESULTS

The dependence of the equilibrium spreading tension of dodecanol crystals (or dodecanol droplets, above ~25°C) on the electrolyte concentration is shown in Figure 4 for all investigated salts. The measurements were done at temperatures ranging from 19 to 26°C; we did a small correction for the temperature variation, assuming surface entropy of 0.138 mN/Km as for neat water, to reduce all data in Figure 4 to a standard temperature of 25°C (from the data, we could estimate the surface entropy of the monolayer to be actually lower by about 30%, which is not a significant difference for our purposes).

The dependence of σ_s on C_m is relatively weak for NaF, NaBr and NaCl – these electrolytes alter σ_s by 1.7 mN/m at most (for comparison, the increment of σ of W|G and W|O in the absence of monolayer is 7-8 mN/m for 5 mol/kg NaCl). This means that the Gibbs adsorption $\Gamma_{el,s}$ of these salts at the monolayer spread around the $C_{12}H_{25}OH$ crystal is relatively small. Surprisingly, the dependence of $\Gamma_{el,s}$ on C_m is non-monotonic for NaBr. This is not what could be expected from the previous studies[57,58,25], which report approximately linear $\sigma_s(C_m)$. The minimum of σ_s means that at low concentration NaBr adsorbs at crystal's spread monolayer, while at high C_m it desorbs. The ion-specific effect we observe with σ_s seems to follow the *reverse* Hofmeister series[59,60] – we find $\sigma_{s,NaBr} > \sigma_{s,NaCl} \approx \sigma_{s,NaF}$ instead of the expected $\sigma_{s,NaBr} < \sigma_{s,NaCl} < \sigma_{s,NaF}$.

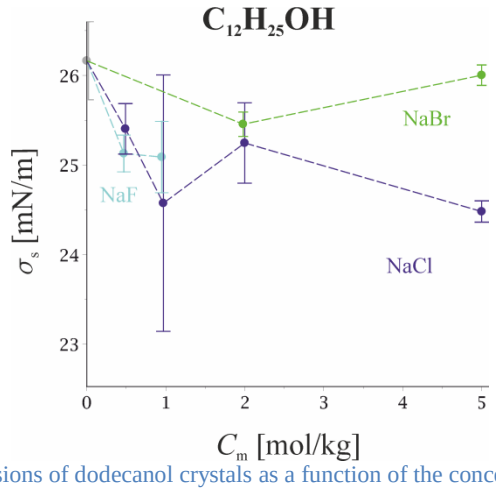

Figure 4. Equilibrium spreading tensions of dodecanol crystals as a function of the concentration C_m of the electrolyte in the substrate, 25°C.

We further measured the surface tension vs. area isotherms for dodecanol monolayers. We rationalized the measurements following a protocol similar to the one we used for the data of Ralston and Healy in the *Theoretical basis* section – we fitted the data with a relatively simple function of the general form:

$$\Gamma^{-1}(\sigma) = \begin{cases} g_1^{\mathrm{LE}} \dfrac{\sigma + g_0^{\mathrm{LE}} + g_{-1}^{\mathrm{LE}}\sigma^{-1} + g_{-2}^{\mathrm{LE}}\sigma^{-2} + g_{-3}^{\mathrm{LE}}\sigma^{-3} + g_{\ln}^{\mathrm{LE}} \ln\left(\sigma/[\mathrm{mN/m}]\right)}{\sigma + g_{\mathrm{d}2}^{\mathrm{LE}}\sigma^2 + g_{\mathrm{d}3}^{\mathrm{LE}}\sigma^3 + g_{\mathrm{d}0}^{\mathrm{LE}}}, & \sigma > \sigma_{\mathrm{t}}; \\ g_1^{\mathrm{LC}}\sigma + g_0^{\mathrm{LC}} & \sigma < \sigma_{\mathrm{t}}. \end{cases} \quad (16)$$

The values of the parameters are tabulated in Table S3&4 for all studied concentrations. The tension ranges from a maximal initial value $\sigma_{\max}$ to the equilibrium σ_s, at which the monolayers collapse. The collapse of long-chain alcohols normally occurs at surface tensions below σ_s (as with the octadecanol in Figure 2), and metastable supersaturated monolayers can live for several hours[48], due to the absence of nuclei for crystallization; in the case of dodecanol, the collapse was in the vicinity of $\sigma = \sigma_s$ (but still slightly lower).

The obtained σ vs. Γ^{-1} isotherms of dodecanol spread on NaCl are shown in Figure 5 (*left*). For dense monolayers, the surface tension decreases with the concentration at fixed Γ. On the opposite, σ increases with C_m for sparse monolayers. The results for NaF are similar, Figure 5 (*right*). The isotherms of NaBr are also qualitatively similar, but quantitatively, the variation of the isotherms is more pronounced, Figure 6. The same data are shown in Figure S10 in coordinates surface pressure $\sigma_0 - \sigma$ vs. area Γ^{-1}, which are more common in the literature (but are not convenient for our purpose – the calculation of the salt adsorption). It is seen there that $\sigma_0 - \sigma$ vs. Γ^{-1} curves stand higher at increased concentration, and they follow the *direct* Hofmeister series: $(\sigma_0 - \sigma)_{\mathrm{NaBr}} > (\sigma_0 - \sigma)_{\mathrm{NaCl}}$. Both findings agree with the literature data[22,25,58].

The effect of the salt on the phase transition is interesting, in the light of the previous reports for significant effect of the electrolyte on the conditions of the phase transition in monolayers[31-33] and bilayers[38]. When the concentration of NaCl or NaF increases, the LE-LC phase transition occurs at higher surface tension σ_t and at higher areas per molecule (Figure 5). NaBr has little effect on σ_t (Figure 6). This suggests that NaBr tend to stabilize the LE phase in comparison with NaCl & NaF. Frumkin and Pankratov reached a similar conclusion (the hydrophobic ion I^- stabilizes the expanded ethylpalmitate film while the hydrophilic SO_4^{2-} stabilizes the condensed film, *fig. 1* in ref [22]).

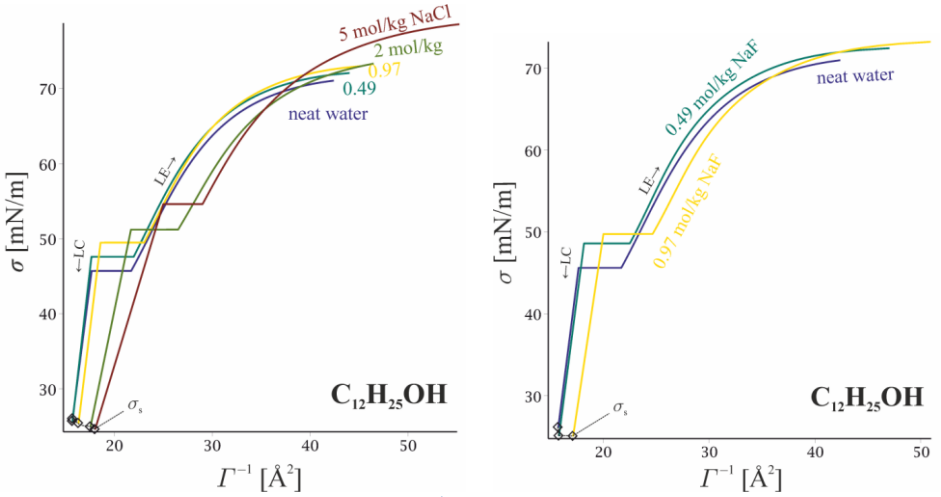

Figure 5. Surface tension σ vs. area per molecule Γ^{-1} for $C_{12}H_{25}OH$ monolayers spread on substrates of various concentrations of NaCl (*left*, T = 24.9±1.1°C) and NaF (*right*, 25.6±0.6°C). Lines are polynomial fits of the inverse dependence $\Gamma^{-1}(\sigma)$ with eq (16); diamonds correspond to the equilibrium spreading pressure of dodecanol crystals (chosen by us as standard state). A 1st order phase transition between *liquid condensed* (LC) and *liquid expanded* (LE) surface phases occurs (the plateaus).

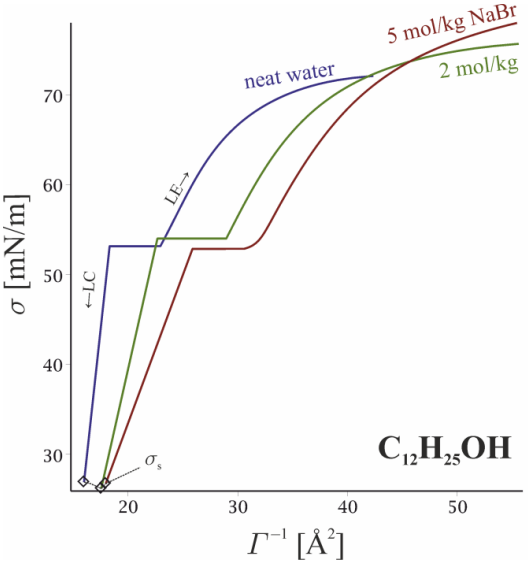

Figure 6. Surface tension σ vs. area Γ^{-1} for $C_{12}H_{25}OH$ monolayers spread on substrates of various concentrations of NaBr at 19.8±1.0°C. Lines are polynomial fits of the data with eq (16); diamonds correspond to the equilibrium spreading pressure of pure dodecanol crystals.

The next step in our method is the calculation of $\Delta_s\mu$. The isotherms (16) and the equilibrium spreading tension data in Figure 4 were used in eq (7) to calculate the chemical potential $\Delta_s\mu$ as a function of σ (the integral can be expressed with standard special functions but we found it easier to evaluate it numerically). With NaCl, we fitted the data for σ_s vs. C_m with a square polynomial, σ_s/[mN/m] = 25.97 – 0.7121C_m/[mol/kg] + 0.08544(C_m/[mol/kg])^2, to smooth it and to avoid the effect that the experimental dispersion has on the numerical differentiation. For NaF & NaBr, the σ_s data were used as they were (only with a small temperature correction, to reduce their values to the average temperature of the compression runs). The obtained $\Delta_s\mu$ vs. σ were then substituted in eq (12) to determine $(d\Delta_s\mu/d\gamma_\pm C_m)_\sigma$ in eq (8) for Γ_{el}.

The resulting Gibbs adsorption Γ_{el} of NaCl at the dodecanol monolayer is shown in Figure 7, as a function of σ (as it follows from eqs (8),(12)&(16)). According to the figure, Γ_{el} is *positive* for C_m = 0.49-2 mol/kg, and it increases proportionally to the salt concentration. Not only for NaCl, but also for the other halides we investigated, the electrolyte adsorption follows

a similar trend with the increase of the adsorption Γ of the surfactant: for dilute LE monolayers, $d\Gamma_{el}/d\Gamma > 0$, until a maximum is reached; for dense LE monolayers, Γ_{el} decreases with Γ. The existence of a maximum of Γ_{el} as a function of Γ was qualitatively noticed by Frumkin and Pankratov[22] (cf. their *footnote 3*). At the point of the phase transition, the LC monolayer adsorbs more salt than the LE film. With the increase of the density of the LC film, the salt adsorption rapidly decreases. The jump that Γ_{el} experiences at the point of the 1st order LE-LC transition (from a smaller positive LE value to a larger LC value) can be compared with the conclusion of Aroti et al.[33], that for the uncharged DPPC monolayer, Γ_{el} is close to zero in the LC phase and $\Gamma_{el} > 0$ in the LE (but their conclusions regarding Γ_{el} are indirect). In Figure S11, the same data are presented in coordinates electrolyte Gibbs adsorption Γ_{el} vs. Γ^{-1} of the surfactant (a parametric plot of eqs (8),(12)&(16) for $\Gamma_{el}(\sigma)$ against eq (16) for $\Gamma^{-1}(\sigma)$). There, the data for the adsorption of 2M KCl at the octadecanol monolayer from Figure 3 are given for comparison – the adsorptions of the two salts at the two monolayers in their common range of areas are of similar order of magnitude.

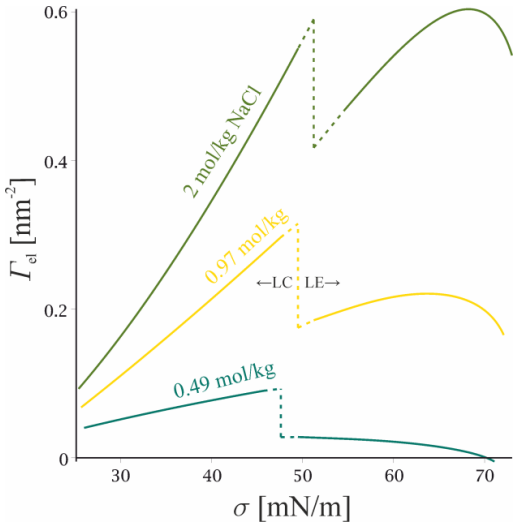

Figure 7. The Gibbs adsorption Γ_{el} of NaCl as a function of the surface tension σ of the dodecanol monolayer. Γ_{el} is calculated using eqs (8),(12)&(16).

The data for the adsorption $\Gamma_{el}^{z=0}$ of NaCl at the ε-discontinuity surface following from eq (14) is shown in Figure 8 as a function of the adsorption Γ of the surfactant (for 0.49 mol/kg NaCl), and in Figure S12 – as a function of Γ^{-1} for the other investigated salt concentrations. In the close vicinity of the collapse, $\Gamma_{el}^{z=0}$ is negative at all concentrations (compare with KCl in Figure 3), but steeply increases upon expansion. For the LE phase, we find $\Gamma_{el}^{z=0} < \Gamma_{el}$, but only at the lowest concentration, 0.49 mol/kg, the adsorption $\Gamma_{el}^{z=0}$ of NaCl is negative (Figure 8); at 0.97 and 2 mol/kg NaCl, $\Gamma_{el}^{z=0} > 0$, i.e. NaCl is *attracted* by the LE film.

When the data is represented in coordinates $\Gamma_{el}^{z=0}$ vs. Γ, it becomes obvious that the extrapolation of the electrolyte adsorption towards monolayers of zero density, $\lim_{\Gamma\to 0}(\Gamma_{el}^{z=0})$, leads approximately to the right value, namely, the physical adsorption $\Gamma_{el\,0}^{z=0}$ of NaCl at the neat W|G surface ($\Gamma_{el\,0}^{z=0}$ is indicated by the horizontal line in Figure 8, cf. Table S1; the dashed line ranging from $\Gamma = 0$ to the LE region is a manual extrapolation). One sees from Figure 8 that $\Gamma_{el}^{z=0}$ increases with the density of the LE phase, except for the region near the phase transition. From the initial slope of the $\Gamma_{el}^{z=0}$ vs. Γ curve, one can estimate that at 0.49 mol/kg NaCl, each 35 surfactant molecules attract one cation and one anion (each 8 at 0.97 mol/kg, each 3 at 2 mol/kg). This numbers can be compared to the finding of Petrache et al.[61], that in vesicles each 60 lipids adsorb one Br^- ion at 0.1M.

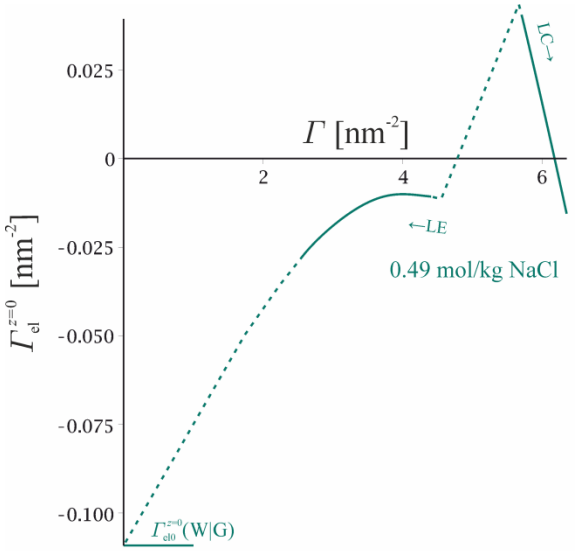

Figure 8. NaCl's adsorption $\Gamma_{el}^{z=0}$ at the surface of $\mathcal{E}$-discontinuity as functions of the surfactant adsorption Γ. This is a parametric plot of $\Gamma_{el}^{z=0}(\sigma)$ against $\Gamma(\sigma)$. The adsorption at $z = 0$ follows from eq (14). The dashed curves are an extrapolation. $\Gamma_{el0}^{z=0}$ is the adsorption of NaCl at the neat W|G surface, cf. S2.

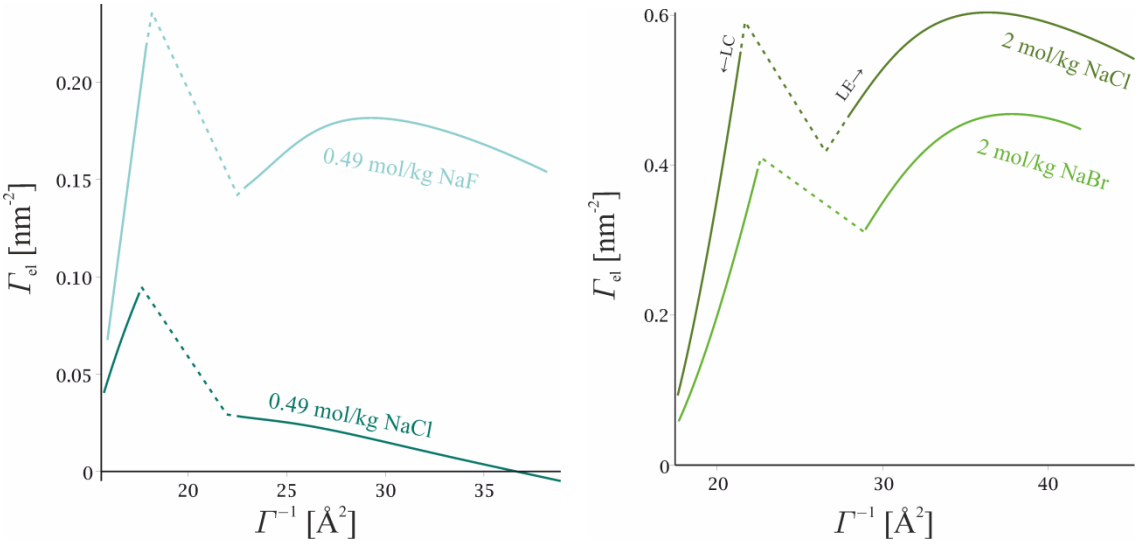

Figure 9. Adsorption Γ_{el} of 0.49 mol/kg NaF & NaCl (*left*) and 2 mol/kg NaCl & NaBr (*right*) at a surface with spread $C_{12}H_{25}OH$ as a function of Γ^{-1}.

Let us now consider the Hofmeister effect on the ion adsorption. In Figure 9 (*left*), we compare the adsorption of NaF & NaCl at the dodecanol monolayer, C_m = 0.49 mol/kg. The uncertainty of the adsorptions obtained was estimated as explained in the *Theoretical basis* section: it is ±0.06 nm^{-2} for NaF and ±0.04 nm^{-2} for NaCl for the whole range of Γ. Since the values of Γ_{el} of these salts are close to zero, the relative error is rather large and in the case of NaCl, even the sign of the Gibbs adsorption is uncertain. Yet, the difference between Γ_{el} of NaF and NaCl is statistically significant (0.10-0.15 nm^{-2}) and one can say that NaF is of higher adsorption than NaCl. In Figure 9 (*right*), we compare the adsorption of NaCl and NaBr at 2 mol/kg. The estimated uncertainty is ±0.05 and ±0.04 nm^{-2} for the three salts, respectively (corresponding to relative errors of about ±20% and ±10%). Thus, instead of the expected direct Hofmeister series, the *reverse* one is followed: for our electroneutral surface, Γ_{el}(NaF) > Γ_{el}(NaCl) > Γ_{el}(NaBr) (note the difference in comparison with the series of the surface pressure, Figure S10). This series can be compared with the rule formulated by Schwierz et al.[60], that the

direct Hofmeister series ($Br^- > Cl^- > F^-$) is valid for negatively charged surfaces, but the reverse series ($F^- > Cl^- > Br^-$) is valid for positively charged surfaces (see also ref [59]).

In all cases, the adsorption of the salt at the monolayer is significantly more positive than the one at neat W|G or W|O interfaces (Table S1). The high Γ_{el} of, for example, NaCl at the monolayer can be due to **(i)** the attraction of the chloride ion to the surfactant layer (corresponding to an electric double layer with Cl^- in the adsorption layer and Na^+ in the diffuse layer); **(ii)** the attraction of Na^+ to the lipid layer (Na^+ dominates in the adsorption layer and Cl^- dominates in the diffuse); and **(iii)** both ions are attracted to the monolayer with about equal force (corresponding to approximately electroneutral adsorption layer and absent diffuse layer). Which of these three cases is actually occurring can be judged from the measurements of the Volta potential ΔV of the monolayer, Figure 10 (*left*). Only the data falling into the LE region are considered (the data at higher adsorptions are complicated by the kinetics of the phase transition). The sign of ΔV is positive, i.e. the alcoholic groups contribute to the surface dipole moment with the positive pole toward the gas phase (as illustrated in Figure 1). ΔV becomes more positive with the increase of the salt concentration C_m. A similar trend is followed by the $\Delta\chi$-potential of 1:1 electrolytes adsorbing at the neat water surface[62,63], and it has been explained with the ion-specific drop of the dielectric permittivity of the solution8. We will now attempt to interpret the data in Figure 10 (*left*) in a similar manner.

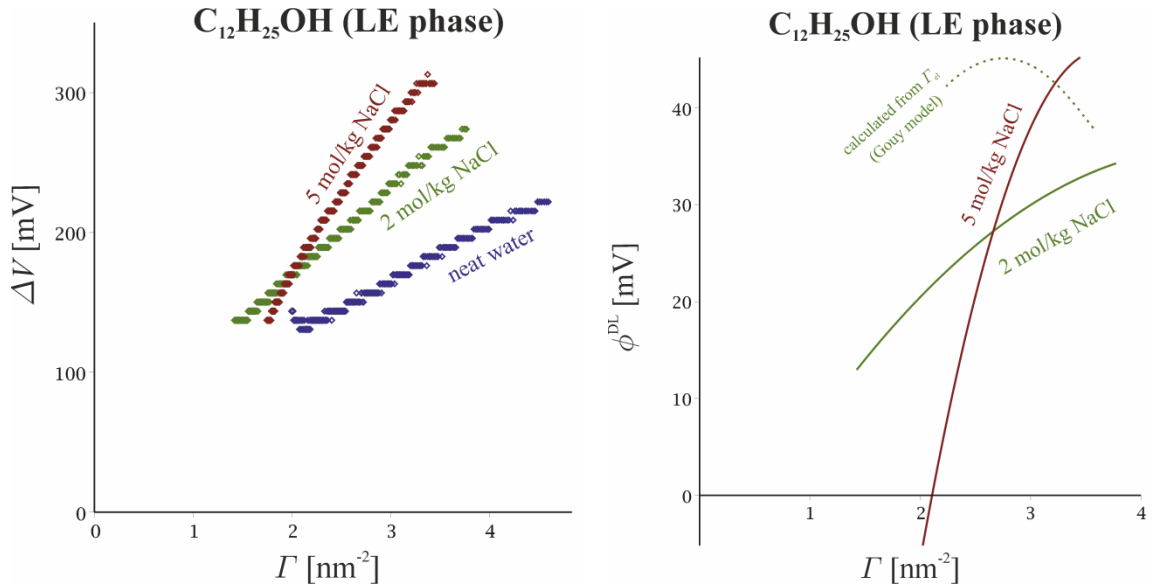

Figure 10. *Left:* Volta potential difference ΔV vs. dodecanol adsorption in the LE phase at 3 different NaCl concentrations. *Right:* the change in the electric double layer potential ϕ^{DL} as a function of the dodecanol adsorption. The potential ϕ^{DL} is calculated from ΔV according to eq (22). The dashed line is calculated using Γ_{el} for 2 mol/kg NaCl from Figure 9 (*right*) through Gouy's equation under the assumption that no anions are specifically adsorbed (cf. S9 for details).

The ΔV-potential of the monolayer is defined with the difference

$$\Delta V \equiv \Delta^G_W\phi(\Gamma) - \Delta^G_W\phi(\Gamma = 0), \quad (17)$$

where $\Delta^G_W\phi(\Gamma)$ is the potential drop through the interface between the gas and the electrolyte solution in the presence of monolayer, and $\Delta^G_W\phi(\Gamma = 0)$ is the drop at the neat surface of the salt solution (the choice of direction is such that positive $\Delta^G_W\phi$ potential corresponds to positive pole of the surface dipole pointing toward the gas). The potential $\Delta^G_W\phi(\Gamma = 0)$ of the neat electrolyte can be expressed as

$$\Delta^G_W\phi(\Gamma = 0) = \chi_0 + \Delta\chi, \quad (18)$$

where χ_0 is $\Delta^G_W\phi$ of neat water in the absence of salt, and $\Delta\chi$ is its change upon addition of electrolyte. The $\Delta\chi$-potential is a measurable quantity – for 2 and 5 mol/kg NaCl, it is about

–3.2 and –17.6 mV, respectively (interpolation of the data of Jarvis and Scheiman[63]). In contrast, the potential drop χ_0 of the surface of the pure water is very hard to measure[64,65]; we use the value8 $\chi_0 = -90$ mV, which agrees with the conclusions of refs [64,65].

Regarding the potential drop $\Delta_{\mathrm{W}}^{\mathrm{G}}\phi(\Gamma)$ at a surface with a monolayer, we assume that it has two additive components – one stemming from the *intrinsic*[56] *surface dipole moment P*, and a second due to the ion distribution (the double layer potential ϕ^{DL}). In the case of W|G with an adsorbed LE monolayer, the intrinsic dipole moment *P* is concentrated predominantly in the vicinity of the interface W|LE between the oily layer and the aqueous electrolyte, where the oriented water molecules and the alcohol polar head groups are located. Thus, the intrinsic dipole moment *P* is concentrated between two dielectrics (note that *P* is partly compensated by a diffuse dipole layer[56] located in the volume of the dielectrics in the vicinity of $z = 0$). Using *eq 55* in ref [56] for the relation between the surface potential drop and *P*, we arrive at the expression:

$$\Delta_{\mathrm{W}}^{\mathrm{G}}\phi(\Gamma) = \frac{L_Q^{\mathrm{W}} + L_Q^{\mathrm{LE}}}{L_Q^{\mathrm{W}}\varepsilon^{\mathrm{W}} + L_Q^{\mathrm{LE}}\varepsilon^{\mathrm{LE}}} P + \phi^{\mathrm{DL}}, \tag{19}$$

where ε^{W} is the dielectric permittivity of the aqueous solution; $\varepsilon^{\mathrm{LE}}$ is the permittivity of the LE layer; L_Q^{W} and L_Q^{LE} are the quadrupolar lengths[56] of the aqueous solution and the LE phase respectively. Since $\varepsilon^{\mathrm{W}} >> \varepsilon^{\mathrm{LE}}$, we can neglect the second term in the denominator of eq (19); eqs (17)-(19) can then be written as:

$$\Delta V(C_{\mathrm{m}}) = \frac{L_Q^{\mathrm{W}} + L_Q^{\mathrm{LE}}}{L_Q^{\mathrm{W}}} \frac{P}{\varepsilon^{\mathrm{W}}(C_{\mathrm{m}})} + \phi^{\mathrm{DL}} - \chi_0 - \Delta\chi\,. \tag{20}$$

The quantity $\varepsilon^{\mathrm{W}} L_Q^{\mathrm{W}}/(L_Q^{\mathrm{W}} + L_Q^{\mathrm{LE}})$ can be identified with the effective surface permittivity ε^{S} used in ref [8]. The dielectric permittivity ε^{W} of the solution is a function of the salt concentration. It has been measured for NaCl up to the solubility limit by Buchner et al.[66] ($\varepsilon^{\mathrm{W}}/\varepsilon_0 = 78.4$, 55.5 and 44.7 for 0, 2 and 5 mol/kg NaCl respectively). The measurement is of quite high uncertainty – for comparison, the data of Barthel et al.[67] for the same electrolyte differ by up to 20%. We also assume that, in the absence of electrolyte, $\phi^{\mathrm{DL}}(C_{\mathrm{m}} = 0)$ is small compared to $\phi^{\mathrm{DL}}(C_{\mathrm{m}})$ (no electric double layer is developed in the absence of ions, i.e. H^+ and OH^- in the pure water are neglected); that the quadrupolar length L_Q^{W} of the solution is independent of C_{m} (cf. *eq 45* in ref [68]); and that the intrinsic surface dipole *P* also does not change with C_{m}. This allows us to write eq (20) for ΔV in the absence of electrolyte as:

$$\Delta V(0) = \frac{L_Q^{\mathrm{W}} + L_Q^{\mathrm{LE}}}{L_Q^{\mathrm{W}}} \frac{P}{\varepsilon^{\mathrm{W}}(0)} - \chi_0\,. \tag{21}$$

We then solve eqs (20)&(21) for *P* and the electric double layer potential ϕ^{DL}. The result for the latter reads:

$$\phi^{\mathrm{DL}}(C_{\mathrm{m}}) = \Delta V(C_{\mathrm{m}}) - \frac{\varepsilon^{\mathrm{W}}(0)}{\varepsilon^{\mathrm{W}}(C_{\mathrm{m}})}\Delta V(0) - \left[\frac{\varepsilon^{\mathrm{W}}(0)}{\varepsilon^{\mathrm{W}}(C_{\mathrm{m}})} - 1\right]\chi_0 + \Delta\chi(C_{\mathrm{m}})\,. \tag{22}$$

This formula is allowing us to calculate ϕ^{DL}. The result is a rather rough approximation for several reasons. The first is the high uncertainties of the values of the quantities in eq (22): the inaccuracy in χ_0 is very high, about ±60 mV; ±5 mV for $\Delta\chi$; ±20% for ε^{W}; and the ΔV-potential we measure varies by ±15 mV from run to run. The second reason is the assumption for the independence of *P* on C_{m} – this dependence might be significant (at least for bromides and iodides[22]). The third is the rough assumption that the electric double layer and the dipolar potentials in eq (19) are additive. Finally, $\phi^{\mathrm{DL}}(C_{\mathrm{m}} = 0)$ might be comparable with $\phi^{\mathrm{DL}}(C_{\mathrm{m}})$. Nevertheless, we expect eq (22) to give the correct sign, order of magnitude and trend with Γ of the double layer potential ϕ^{DL}.

The dependence of ϕ^{DL} on Γ that follows from eq (22) is illustrated in Figure 10 (*right*). The order of magnitude is correct – this can be shown by comparing ϕ^{DL} with the estimation that follows from the value of the adsorption of NaCl at 2 mol/kg in Figure 7 combined with Gouy's equation (as described in S9; note that Gouy's model is a very crude approximation for the considered system). The sign of ϕ^{DL} suggests that for NaCl, it is the *sodium ion*, and not Cl^-, that is actually attracted by the monolayer. Thus, the monolayer must be positively charged in the presence of NaCl. The reverse Hofmeister series observed with the adsorption of NaF, NaCl and NaBr suggests that the same conclusion is valid for these three electrolytes, according to the rule of Schwierz et al.[60] (although with NaBr, we expect significant hydrophobic attraction of Br^- in addition to the adsorption of Na^+).

Our tentative explanation of these observations is that the adsorption of Na^+ is caused by the interaction of the electrolyte with the intrinsic surface dipole moment P. In the absence of a monolayer, the surface potential is about −90 mV (corresponding to positive pole of the surface dipole pointing toward the aqueous electrolyte and attracting the anions, Figure 1). The alcohol adsorption results in ΔV of the order of +150-300 mV, i.e. $C_{12}H_{25}OH$ reverses the dipole moment and for the monolayer (the *negative* pole points toward the solution and it attracts the *cations*, Figure 1). This hypothesis is in agreement with the observed trend of the ϕ^{DL} vs. Γ curve: as the surfactant adsorption decreases, the surface approaches the point $\Gamma_{P=0}$ *of zero dipole*[56]. Assuming that $\Gamma_{P=0}$ corresponds to $\Delta_W^G\phi(\Gamma) = \Delta V + \chi_0 + \Delta\chi = 0$, by extrapolation of the data in Figure 10 (*left*), we can estimate it at about $\Gamma_{P=0}$ = 0.5-1.5 nm^{-2} (increasing with C_m). If the surface dipole causes the ion adsorption, Γ_{el} and ϕ^{DL} should decrease as Γ approaches $\Gamma_{P=0}$, as is indeed observed. It is also interesting to compare the point of zero dipole (where $\Delta_W^G\phi = 0$) with the point of zero charge $\Gamma_{e=0}$ (where $\phi^{DL} = 0$). Although probably very inaccurate, Figure 10 (*right*) allows it to be estimated at about $\Gamma_{e=0} \approx 2$ nm^{-2} at C_m = 5 mol/kg, and at $\Gamma_{e=0} \approx 0.7$ nm^{-2} at 2 mol/kg NaCl. Thus, the values of Γ corresponding to zero charge and zero surface dipole are close, and have similar trend with the increase of C_m. Since $\Gamma_{e=0} > \Gamma_{P=0}$, at the point of zero dipole, the electric double layer is negatively charge ($\phi^{DL} < 0$), i.e. in the absence of surface dipole moment, the anions are attracted to the monolayer more strongly than the cations.

We sought for indications in the literature that confirm the relation between the surface dipole moment and the double layer potential. Frumkin and Pankratov[22] suspected significant interaction between the ions and the surface dipole moment, but of qualitatively different nature (they hypothesized that the anions are able to polarize significantly the surface). One interesting phenomenon that finds a simple explanation in the above-stated mechanism of ion-surface interaction is the anomalous dependence of the equilibrium foam film thickness of a film of NaCl solution stabilized with pentanol, reported by Qu et al.[69]. At fixed salt concentration (1 mM NaCl), the increase of the pentanol concentration from 0.001 mM to 1 mM leads to decreased equilibrium thickness (i.e. to decreased electrostatic disjoining pressure and decreased specifically adsorbed charge). The further increase of the pentanol concentration from 1 mM to 10 mM leads to *increased* thickness, i.e. increased electrostatic disjoining pressure and adsorbed charge. In view of our findings, the explanation seems to be that, at low concentrations of the pentanol where $\Gamma < \Gamma_{P=0}$, the average surface dipole still points with the positive pole toward the liquid and leads to adsorption of Cl^-. With the increase of the pentanol concentration, the system approaches the point of zero dipole. When P = 0, the electrostatic disjoining pressure reaches its minimum. As pentanol concentration increases further, the dipole at the surface becomes increasingly negative towards the solution, leading to specific adsorption of Na^+ and to the observed increase of the disjoining pressure and the film thickness.

Other researchers have also argued that small cations can adsorb at uncharged monolayers. According to Petelska and Figaszewski[70], it is the potassium ion, not the chloride, that is

specifically adsorbed at the DPPC monolayer in contact with KCl solution. Similarly, Leontidis et al.[37] needed a specific adsorption of Na^+ in their model for the effect of NaF on DPPC monolayers. Both groups assumed that this interaction is due to ion-specific complexation of the cation and the head group of the lipid. We tend instead to the hypothesis that the attraction is not specific to the DPPC polar head group – it is due to the total intrinsic surface dipole moment P.

Let us stress that eq (19) has been derived for insulators only[56], and the presence of ions of concentration 5 mol/kg will alter it. A generalization of Gouy's equation is required for the quantitative understanding and as a more rigorous test of the results in Figure 10. This generalization should account for the quadrupolarizability of the medium, due to the conjugation between bulk quadrupolarization and surface dipole moment[81]. The problem is beyond the scope of this work, and therefore, the preliminary results we report here should be considered with caution.

CONCLUSIONS

The most important contribution of this work is the method we developed for the determination of the salt adsorption Γ_{el} at a surface of an electrolyte solution with a spread insoluble monolayer (based on the ideas of Frumkin and Pankratov[21]). The method combines data for the surface tension vs. area Γ^{-1} per surfactant molecule with data for the equilibrium spreading tension of the surfactant crystals at several salt concentrations C_m to extract the dependence of Γ_{el} on Γ and C_m, based on the strict themodynamic relations (7)&(8). We demonstrated the capabilities of the method with literature data for octadecanol on KCl substrates and with data measured by us for dodecanol films on solutions of several sodium halides. The method is flexible and can be used for a variety of systems – e.g., one generalization involving only minor changes that is particularly interesting for us is the application of the method to insoluble monolayers of ionic surfactants.

The most interesting results obtained with the new method are:

(i) The adsorption Γ_{el} of all studied electrolytes (KCl, NaF, NaCl, NaBr) at a surface with a dense alkanol monolayer is significantly larger than the adsorption at neat W|G or W|O (e.g., Figure 8). This means that an attractive force exists that acts between one or both of the ions and the alcohol monolayer, absent at the neat interfaces.

(ii) Γ_{el} is changing significantly with the density of the dodecanol monolayer, following a non-monotonous and discontinuous pattern. For the salts and the concentrations we investigated, the salt adsorption typically reaches a maximum as a function of Γ in the LE region (e.g., Figure 7) – this confirms the qualitative conclusions of Frumkin and Pankratov[22]. At the point of the phase transition, Γ_{el} jumps to a higher LC value, but then, near the point of collapse, steeply decreases to a much smaller, even negative adsorption.

(iii) Γ_{el} at the monolayer is an approximately linear function of the salt concentration at most areas per surfactant molecule.

(iv) The adsorption at the dodecanol monolayers is ion-specific and follows the reverse Hofmeister series $\Gamma_{el}(NaF) > \Gamma_{el}(NaCl) > \Gamma_{el}(NaBr)$. According to the rule of Schwierz et al.[60], this is indicative of positively charged surface, i.e. Na^+ is probably the specifically adsorbed ion while the anions remain in the diffuse layer.

To analyse further the distribution of the two ions in the vicinity of the monolayer, we measured its Volta potential ΔV at several concentrations of NaCl. We assumed that the electrolyte affects the Volta potential by altering the dipolar contribution to it (through the altered dielectric permittivity ε^W of the concentrated solution, as in ref [8]) and by forming an

electric double layer of potential ϕ^{DL}. We could estimate the first effect (which is dominating) to extract the value of ϕ^{DL} (Figure 10). The result is in agreement with *positive* double layer potential, i.e. indeed, the sodium ion is located in the adsorption layer while Cl^- remains in the diffuse layer.

These results are not easy to explain with the published models[4-5,6-8,15-20] of the electrolyte adsorption involving image, hydration, van der Waals and hydrophobic interaction. The image, the hydration and the hydrophobic forces are not expected[7] to change significantly in the presence of a monolayer. The van der Waals force is roughly proportional to the difference between the Hamaker constant A^H of the hydrophobic phase and A^W of the aqueous solution. In the absence of a monolayer ($A^H = 0$), this force should be repulsive and for a dense monolayer (A^H of the liquid expanded approximately equal to A^W) it is expected to be close to zero[7]. A^H is proportional to the density in the monolayer, and this density is not changing significantly: for the LE monolayer of $C_{12}H_{25}OH$ it was estimated[45] at 810 kg/m^3, and for the LC phase it is 855 kg/m^3 (compare to the density of dodecane, 750 kg/m^3). These small changes are unlikely to cause the complicated dependence of Γ_{el} on Γ we observed. Thus, we conclude that the published models of ion adsorption are missing a major player, that we tentatively identify as the ion-surface dipole interaction. At the neat W|G, the surface dipole moment should attract the anions; the adsorbed alcohol changes the sign of the surface dipole (Figure 1), leading to the adsorption of Na^+ at the monolayer.

ACKNOWLEDGEMENT. The work is funded by National Science Fund through Contract 51 from 12.04.2016 with Sofia University. The authors are grateful to the H2020 project Materials Networking. We thank Prof. John Ralston for sharing some unpublished data with us, and Prof. Tzvetanka Ivanova for assistance with the experimental techniques used in this study.

SUPPORTING INFORMATION. 1. List of symbols and abbreviations. **2.** Tensiometric data for the neat surfaces of the salt solutions. **3.** Equilibrium spreading tension of $C_{18}H_{37}OH$ crystals and chemical potential of the monolayer. **4.** Correction of the apparent area per molecule for the solubility of the monolayer and for the kinetic barrier for the LE-LC phase transition. **5.** Parameters of the regression of the σ vs. Γ data. **6.** The reverse thermodynamic problem. **7.** Kinetics of spreading of the monolayer around dodecanol crystals. **8.** Concentration and Hofmeister effects on dodecanol monolayers: additional figures. **9.** Comparison of the experimental potential ϕ^{DL} of the electric double layer and the electrolyte adsorption within Gouy's model. **10.** Additional references.

REFERENCES

1. Aveyard, R.D.; Saleem, S.M. Interfacial tensions at alkane-aqueous electrolyte interfaces. *J. Chem. Soc. Faraday Trans. 1* **1976**, *72*, 1609–1617.
2. Langmuir, I. The constitutions and fundamental properties of solids and liquids. *J. Am. Chem. Soc.* **1917**, *39*, 1848–1906.
3. Aveyard, R.; Saleem, S.M. Work and entropy of adhesion at liquid–liquid interfaces and the relationship to salt desorption. *J. Chem. Soc. Faraday Trans. 1* **1977**, *73*, 896-904.
4. Onsager, L.; Samaras, N.N.T. The surface tension of Debye-Hückel electrolytes. *J. Chem. Phys.* **1934**, *2*, 528–536.

5. Schmutzer, E. Zur Theorie der Oberflächenspannung von Lösungen. *Z. Phys. Chem. (Leipzig)* **1955**, *204*, 131−156.
6. Slavchov, R.I.; Novev, J.K. Surface tension of concentrated electrolyte solutions. *J. Colloid Interface Sci.* **2012**, *387*, 234−243.
7. Slavchov, R.I.; Peshkova, T.V. Adsorption of ions at the interface oil|aqueous electrolyte and at interfaces with adsorbed alcohol. *J. Colloid Interface Sci.* **2014**, *428*, 257−266.
8. Slavchov, R.I.; Novev, J.K.; Peshkova, T.V.; Grozev, N.A. Surface tension and surface $\Delta\chi$-potential of concentrated Z_+:Z_- electrolyte solutions. *J. Colloid Interface Sci.* **2013**, *403*, 113−126.
9. Martens, L.K., ed. *Technical encyclopedia*, Vol. 10. OGIZ, Moscow, 1933 (in Russian).
10. Jungwirth, P.; Tobias, D.J. Specific ion effects at the air/water interface. *Chem. Rev.* **2006**, *106*, 1259−1281.
11. Ghosal, S.; Hemminger, J.C.; Bluhm, H.; Mun, B.S.; Hebenstreit, E.L.D.; Ketteler, G.; Ogletree, D.F.; Requejo, F.G.; Salmeron, M. Electron spectroscopy of aqueous solution interfaces reveals surface enhancement of halides. *Science* **2005**, *307*, 563−536.
12. Liu, D.; Ma, G.; Levering, L.M.; Allen, H.C. Vibrational spectroscopy of aqueous sodium halide solutions and air-liquid interfaces. *J. Phys. Chem. B* **2004**, *108*, 2252−2260.
13. Sloutskin, E.; Baumerta, J.; Ocko, B.M.; Kuzmenko, I.; Checco, A.; Tamam, L.; Ofer, E.; Gog, T.; Gang, O.; Deutsch, M. The surface structure of concentrated aqueous solutions. *J. Chem. Phys.* **2007**, *126*, 054704.
14. Lima, E.R.A.; de Melo, B.M.; Baptista, L.T.; Paredes, M.L.L. Specific ion effects on the interfacial tension of water/hydrocarbon systems. *Brazil. J. Chem. Eng.* **2013**, *30*, 55−62.
15. Ivanov, I.B.; Marinova, K.G.; Danov, K.D.; Dimitrova, D.; Ananthapadmanabhan, K.P.; Lips, A. Role of the counterions on the adsorption of ionic surfactants. *Adv. Colloid Interface Sci.* **2007**, *134–135*, 105–124.
16. Ivanov, I.B.; Slavchov, R.I.; Basheva, E.S.; Sidzhakova, D.; Karakashev, S.I. Hofmeister effect on micellization, thin films and emulsion stability. *Adv. Colloid Interface Sci.* **2011**, *168*, 93–104.
17. Boström, M.; Kunz, W.; Ninham, B.W. Hofmeister effects in surface tension of aqueous electrolyte solution. *Langmuir* **2005**, *21*, 2619–2623.
18. Parsons, D.F.; Ninham, B.W. Nonelectrostatic ionic forces between dissimilar surfaces. *J. Phys. Chem. C* **2012**, *116*, 7782–7792.
19. Santos, A.P.; Levin, Y. Ions at the water–oil interface. *Langmuir* **2012**, *28*, 1304-1308.
20. Levin, Y. Polarizable ions at interface. *Phys. Rev. Lett.* **2009**, *102*, 147803.
21. Leontidis, E. Chaotropic salts interacting with soft matter: beyond the lyotropic series. *Current Opinion Colloid Interface Sci.* **2016**, 23, 100−109.
22. Frumkin, A.; Pankratov, A. Properties of monomolecular layers on solutions of salts II. *Acta Physicochim. URSS* **1939**, *10*, 55–64.
23. Adam, N.K. *The physics and chemistry of surfaces*. Clarendon Press, 1941.

24. Langmuir, I. Oil lenses on water and the nature of monomolecular expanded films. *J. Chem. Phys.* **1933**, *1*, 756–776.
25. Ralston, J.; Healy, T.W. Specific cation effects on water structure at the air-water and air-octadecanol monolayer-water interfaces. *J. Colloid Interface Sci.* **1973**, *42*, 629–644.
26. Aveyard, R.; Saleem, S.M.; Heselden, R. Desorption of electrolytes at liquid–vapour and liquid–liquid interfaces. *J. Chem. Soc. Faraday Trans. 1* **1977**, *73*, 84–94.
27. Karraker, K.A.; Radke, C.J. Disjoining pressures, zeta potentials and surface tensions of aqueous non-ionic surfactant/electrolyte solutions: theory and comparison to experiment. *Adv. Colloid Interface Sci.* **2002**, *96*, 231–264.
28. Penfold, J.; Staples, E.; Tucker, I.; Thompson, L.; Thomas, R.K. The adsorption of non-ionic mixtures at the air-water interface. *J. Colloid Interface Sci.* **2002**, *247*, 404–411.
29. Harkins, W.D.; Morgan, J.W. Polymolecular and monomolecular films. *Proc. Nat. Acad. Sci.* **1925**, *11*, 637–643.
30. Langmuir, I.; Schaefer, V.J. The effect of dissolved salts on insoluble monolayers. *J. Am. Chem. Soc.* **1937**, *59*, 2400–2414.
31. Pankratov, A. Properties of monomolecular layers on solutions of salts I. *Acta Physicochim. URSS* **1939**, *10*, 45–54.
32. Shibata, A.; Yamashita, S.; Yamashita, T. Specific anion effect on water structure at polypeptide monolayer-water interface. *Bull. Chem. Soc. Jpn.* **1982**, *55*, 2814–2819.
33. Aroti, A.; Leontidis, E.; Maltseva, E.; Brezesinski, G. Effects of Hofmeister anions on DPPC Langmuir monolayers at the air−water interface. *J. Phys. Chem. B* **2004**, *108*, 15238–15245.
34. Weil, I. Surface concentration and the Gibbs adsorption law. *J. Phys. Chem.* **1966**, 70, 133–140.
35. Goddard, E.D.; Kao, O.; Kung, H.C. Counterion effects in charged monolayers. *J. Colloid Sci.* **1968**, *27*, 616–624.
36. Petrache, H.I.; Tristram-Nagle, S.; Harries, D.; Kučerka, N.; Nagle, J.F.; Parsegian, V.A. Swelling of phospholipids by monovalent salt. *J. Lipid Res.* **2006**, *47*, 302–309.
37. Leontidis, E.; Aroti, A. Liquid expanded monolayers of lipids as model systems to understand the anionic Hofmeister series 2. *J. Phys. Chem. B* **2009**, *113*, 1460–1467.
38. Cunningham, B.A.; Shimotake, J.E.; Tamura-Lis, W.; Mastran, T.; Kwok, W.-M.; Kauffman, J.W.; Lis, L.J. The influence of ion species on phosphatidylcholine bilayer structure and packing. *Chem. Phys. Lipids* **1986**, *39*, 135–143.
39. Slavchov, R.I.; Novev, J.K. Comment on "Surface tension of concentrated electrolyte solutions". *J. Colloid Interface Sci.* **2014**, *423*, 168–169.
40. Nishikido, N.; Matuura, R. The effect of added inorganic salts on the micelle formation of nonionic surfactants in aqueous solutions. *Bull. Chem. Soc. Jpn.* **1977**, *50*, 1690–1694.
41. Hamer, W.J.; Wu, Y.-C. Osmotic coefficients and mean activity coefficients of uni-univalent electrolytes in water at 25°C. *J. Phys. Ref. Data* **1972**, *1*, 1047–1099.
42. Smith, R.D.; Berg, J.C. The collapse of surfactant monolayers at the air—water interface. *J. Colloid Interface Sci.* **1980**, *74*, 273–286.

43. Bernett, M.K.; Jarvis, N.J.; Zisman, W.A. Properties of monolayers of (omega)-monohalogenated fatty acids and alcohols adsorbed on water. *J. Phys. Chem.* **1964**, *68*, 3520–3529.
44. Defay, R.; Prigogine, I. *Surface tension and adsorption*. Longmans, Green and Co., London, 1966.
45. Casson, B.D.; Braun, R.; Bain, C.D. Phase transitions in monolayers of medium-chain alcohols on water studied by sum-frequency spectroscopy and ellipsometry. *Faraday Discuss.* **1996**, *104*, 209–229.
46. Fainerman, V.B.; Miller, R.; Aksenenko, E.V.; Makievski, A.V. In: Fainerman, V.B.; Möbius, D.; Miller, R., eds. *Surfactants - chemistry, interfacial properties, applications*. Elsevier, 2001, Chapter 3.
47. Ferrari, M.; Ravera, F.; Liggieri, L.; Motschmann, H.; Yi, Z.; Krägel, J.; Miller, R. Adsorption and surface rheology of n-dodecanol at the water/air interface. *J. Colloid Interface Sci.* **2004**, *272*, 277–280.
48. Brooks, J.H.; Alexander, A.E. *The spreading behavior and crystalline phases of fatty alcohols*. In: la Mer, V.K., ed. *Retardation of evaporation by monolayers: transport processes*. Academic press, New York & London, 1962.
49. O'Brien, R.N.; Feher, A.I.; Leja, J. Spreading of monolayers at the air—water interface. *J. Colloid Interface Sci.* **1976**, *56*, 474–482.
50. Hua, W.; Verreault, D.; Adams, E.M.; Huang, Z.; Allen, H.C. Impact of salt purity on interfacial water organization revealed by conventional and heterodyne-detected vibrational sum frequency generation spectroscopy. J. Phys. Chem. C **2013**, *117*, 19577−19585.
51. Lunkenheimer, K.; Pergande, H.-J.; Krüger, H. Apparatus for programmed high-performance purification of surfactant solutions. Rev. Sci. Instrum. **1987**, *58*, 2313-2316.
52. Shapovalov, V.L.; Möhwald, H.; Konovalov, O.V.; Knecht, V. Negligible water surface charge determined using Kelvin probe and total reflection X-ray fluorescence techniques. *Phys. Chem. Chem. Phys.* **2013**, *15*, 13991-13998.
53. Lange, H.; Jeschke, P. In: Schick, M.J., ed. *Nonionic surfactants. Physical chemistry*. Marcel Dekker Inc., New York, 1987.
54. Bois, A.G.; Panaiotov, I.I.; Baret, J.F. Relaxation in LE-LC transition of fatty acid monolayers. *Chem. Phys. Lipids* **1984**, *34*, 265–277.
55. McConnell, H.M. Structures and transitions in lipid monolayers at the air-water interface. *Ann. Rev. Phys. Chem.* **1991**, *42*, 171–195.
56. Slavchov, R.I.; Dimitrova, I.M.; Ivanov, T. The polarized interface between quadrupolar insulators. *J. Chem. Phys.* **2015**, 143, 154707.
57. Donnison, J.A.; Heymann, E. The equilibrium spreading pressure of oleic acid and of ethyl sebacate on concentrated salt solutions. *Trans. Faraday Soc.* **1946**, *42*, 1–5.
58. Gilby, A.R.; Heymann, E. Oleic acid monolayers on concentrated salt solutions. *Australian J. Sci. Research* **1952**, *5*, 160−172.
59. Slavchov, R.I.; Karakashev, S.I.; Ivanov, I.B. In: Römsted, L., ed. *Surfactant science and technology: retrospects and prospects*. CRC Press - Taylor and Francis, LLC, 2014.

60. Schwierz, N.; Horinek, D.; Netz, R.R. Reversed anionic Hofmeister series: the interplay of surface charge and surface polarity. *Langmuir* **2010**, *26*, 7370–7379.
61. Petrache, H.I.; Zemb, T.; Belloni, L.; Parsegian, V.A. Salt screening and specific ion adsorption determine neutral-lipid membrane interactions. *Proc. Nat. Acad. Sci.* **2006**, *103*, 7982–7987.
62. Frumkin, A. Phase-boundary forces and adsorption at the interface air: solutions of inorganic salts. *Z. Phys. Chem.* **1924**, *109*, 34–38.
63. Jarvis, N.L.; Scheiman, M.A. Surface potentials of aqueous electrolyte solutions. *J. Phys. Chem.* **1968**, *72*, 74–78.
64. Parfenyuk, V.I. Surface potential at the gas–aqueous solution interface. *Colloid J.* **2002**, *64*, 588–595.
65. Kochurova, N.N.; Noskov, B.A.; Rusanov, A.I. Investigation of the surface potential characteristics on a jet of water. *Dokl. Akad. Nauk SSSR* **1976**, *227*, 1386.
66. Buchner, R.; Hefter, G.T.; May, P.M. Dielectric relaxation of aqueous NaCl solutions. *J. Phys. Chem. A* **1999**, *103*, 1–9.
67. Barthel, J.M.G.; Krienke, H.; Kunz, W. In: Bamgärtel, H.; Franck, E.U.; Grünbein, W., eds. *Physical Chemistry of Electrolyte Solutions*. Steinkopff, Darmstadt, 1998.
68. Slavchov, R.I. Quadrupole terms in the Maxwell equations: Debye-Hückel theory in quadrupolarizable solvent and self-salting-out of electrolytes. *J. Chem. Phys.* **2014**, *140*, 164510.
69. Qu, X.; Wang, L.; Karakashev, S.I.; Nguyen, A.V. Anomalous thickness variation of the foam films stabilized by weak non-ionic surfactants. *J. Colloid Interface Sci.* **2009**, *337*, 538–547.
70. Petelska, A.D.; Figaszewski, Z.A. The equilibria of lipid–K^+ ions in monolayer at the air/water interface. *J. Membrane Biol.* **2011**, *244*, 61–66.

Adsorption of ions at uncharged insoluble monolayers: supporting information

CONTENTS

1. LIST OF SYMBOLS AND ABBREVIATIONS

A	area covered by the monolayer
A_0	area covered by the monolayer in the initial moment
C_{el}	particle concentration of the electrolyte [m^{-3}]
C_M	molar concentration of the electrolyte [M]
C_m	molal concentration of the electrolyte [mol/kg]
C_{eq}	equilibrium concentration of the surfactant
D	diffusion coefficient of the surfactant
DPPC	dipalmitoylphosphatidylcholine
g	regression coefficients in eqs (9)&(16)
J	$= \int_0^t \frac{1}{\Gamma} \exp\left(\frac{\Delta_s \mu}{T}\right) dt$
j_D	diffusion flux of surfactant from the surface to the bulk
k	rate constant for desorption
k_s	adjusted rate constant, eq S(6)
K_a	adsorption constant of the surfactant
L_Q^{LE}	quadrupolar length of the LE film
L_Q^{W}	quadrupolar length of the aqueous solution
LC	liquid condensed phase of the monolayer
LE	liquid expanded phase of the monolayer
M_w	molar mass of water
n	amount of dodecanol in the monolayer [mol]
n_0	amount of dodecanol in the monolayer in the initial moment [mol]
P	intrinsic surface dipole moment
T	thermodynamic temperature, T[J] = $k_B T$[K]
t	time
V_{el}	partial molecular volume of the electrolyte
ΔV	surface Volta potential
z^S	shift of the Gibbs surface

Γ	adsorption of the surfactant
Γ_{el}	Gibbs adsorption of the electrolyte
Γ_{el0}	Gibbs adsorption of the electrolyte in the absence of monolayer
$\Gamma_{el}^{z=0}$	adsorption of the electrolyte at the surface of discontinuity of ε
$\Gamma_{el,s}$	Gibbs adsorption of the electrolyte at crystal's spread layer
Γ_t	adsorption of the surfactant at the point of phase transition
$\gamma_\pm$	mean activity coefficient of the electrolyte
γ^S	surface activity coefficient of the surfactant
γ_w	osmotic coefficient
ε^{LE}	dielectric permittivity of the LE film
ε^W	dielectric permittivity of the aqueous solution
μ	chemical potential of the surfactant monolayer
μ_0	standard chemical potential
μ_{el}	chemical potential of the electrolyte
μ_s	chemical potential of the surfactant crystal
$\Delta_s\mu$	$= \mu - \mu_s$
σ	surface or interfacial tension
σ_0	surface tension of the neat electrolyte solution
σ_s	the value of σ for crystal's spread monolayer
σ_t	the value of σ at the point of LE-LC phase transition
χ	surface potential of the electrolyte solution
χ_0	surface potential of pure water
$\Delta\chi$	surface potential increment, $\Delta\chi = \chi - \chi_0$
Φ	$= \exp(-e\phi^{DL}/T)$
ϕ^{DL}	potential drop in the electric double layer
$\Delta_W^G\phi(\Gamma)$	potential drop through W|G in the presence of a monolayer

2. TENSIOMETRIC DATA FOR THE NEAT SURFACES OF THE SALT SOLUTIONS

In Figure S1, we compare the surface tension of sodium halides at W|G and W|alkane interfaces (literature data), which were the motivation for this work, cf. the *Introduction*.

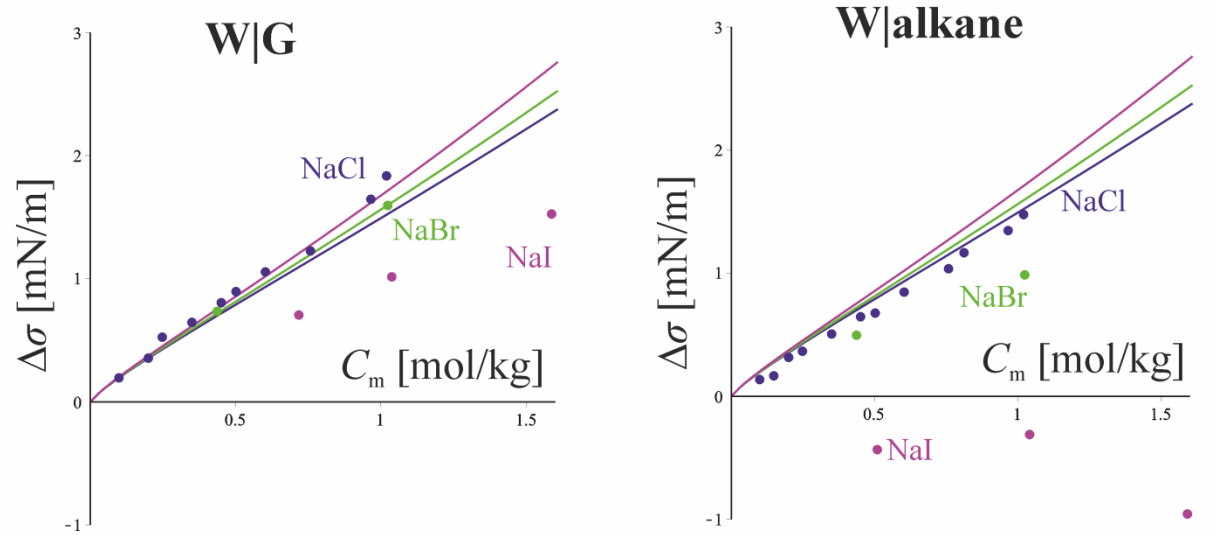

Figure S1. Comparison of the surface tension increment with the concentration of sodium halides at W|G and W|alkane. Data from refs [**1**,**3**,**9**,14]. Lines: theory involving image and hydration forces only[**6**·**7**].

The tension σ_0 of the neat surface of the electrolyte solution must be known for the utilization of our method for determination of Γ_{el}. In most cases, we preferred to use the averaged literature data for σ_0 (the sources in Table S1 were used), because the techniques we use are of better accuracy when the surface tension of the monolayer is measured relative to the one of the neat surface. We did, however, a set of measurements of σ_0 – this is an important test of the purity of the salts and the efficiency of the rinsing procedure we are using to clean the surface from impurities before each measurement. The problem with the foulants is most significant at the highest salt concentrations we investigate (C_m = 5 mol/kg) and in the absence of dodecanol (Γ = 0). This is because **(i)** if the water is clean, the concentration of impurities in the solution is proportional to C_m; **(ii)** the salting-out effect of the dissolved salt on the impurities results into an increase of their surface activity; **(iii)** even at the lowest density Γ of the spread monolayer we are investigating, the monolayer composition is dominated by the dodecanol – less free surface area is available for the impurities when dodecanol is present, and in addition, the data for the adsorption kinetics in S4 below suggest that the dense monolayer results into an energetic barrier for adsorption of the impurities, thus slowing down their effect. Therefore, if we can prove that our cleaning procedure resolves the impurity problem in the worst case – the neat surface of the 5 mol/kg solution, then we guarantee it is working also with the lower concentrations and in the presence of a dodecanol monolayer.

The main measure we did against impurities was rinsing of the surface with a barrier (a variant of one of the most widely used method in the literature[51,52]), which we did before each compression run, and before each measurement of the spreading tension of crystals. The barrier passes through the whole surface, compressing the impurities within a small area; then either some of the liquid in the vicinity of the surface was poured out of the vessel or was sucked with a pump. We tested the effectiveness of this procedure with the pure water and the most concentrated salt solutions by measuring the surface tension as function of the number of rinses (as in Figure S2).

We first tested the cleaning procedure with water. Without the rinsing, we measured surface tension of 72.0±0.14 mN/m. This value is the average of 7 measurements with several batches of water (with a temperature correction reducing all measured values to 25°C). Some of the measurements gave σ_0 as low as 71.8 mN/m. The value after one or more rinses was 72.1±0.06 (compared to the literature value of 72.19 mN/m). It did not vary with the number of rinses after the first one. The cited measurements refer to 120-500 s after the Pt plate was dipped into the liquid, which is the order of magnitude of the time between the end of the last rinse and the end of the compression run in each monolayer experiment of ours (typically, the complete compression run took 2 min, cf. S4).

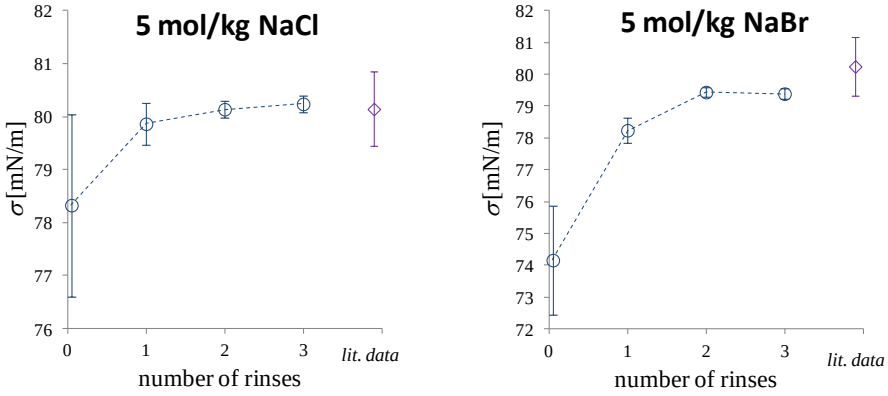

Figure S2. Surface tension of 5 mol/kg NaCl (*left*) and NaBr (*right*) a function of the number of rinses (circles). The averaged literature value is given for comparison (diamond).

The tests with the NaCl (99.8% pure) are summarized in Figure S2 (*left*). Before the first rinse, the value was 78.3±1.7 mN/m. After one (79.9±0.4 mN/m) or more rinses (80.2±0.2 mN/m), the measured σ_0 agreed excellently with the literature values (80.1±0.7 mN/m according to Faktor and Rusanov[44], Pavlov[44], Jarvis and Scheiman[63], and Ozdemir et al.[74] – interpolated values reduced to 25°C). All values refer for 500-600 s after the rinsing. There was a weak tendency for decrease of the measured tension with time after the first rinse, but after the second, the value would not change with more than 0.2 mN/m even after 20-30 min (enough to make even the slower compression runs at lower barrier velocities).

We made the same test with NaCl (99.8% pure) which was baked for 5 h at 615°C. This procedure had only limited effect (as observed also by Hua et al.[50]) and the surface still needed rinsing. We therefore prefer rinsing instead of baking. We finally repeated the same test with NaCl 99.999%. To our surprise, we found this salt contains a very significant amount of surface active impurities (σ = 76.5 mN/m after 360 s, and continued to decrease with time). Therefore, the 99.8% salt was preferred.

The tests with the NaBr (99% pure) lead to very similar results, Figure S2 (*right*). Two rinses are enough to reach the literature value (which is a bit uncertain; our 79.4±0.4 mN/m is slightly higher than Jarvis and Schieman's[63] 79.2 mN/m and slightly lower than Faktor and Rusanov's[44] 80.9 – interpolated values reduced to 25°C). Our values were again quite stable with time (less than 0.2 mN/m drop for 10-20 min), which is enough for a full compression run to be made.

We previously6 measured the tensions of several salts at lower concentration (~1 mol/kg); there, the impurity problem is indeed smaller, i.e. the impurities are stemming from the salt.

We made experiments with 99% NaI as well, including spreading tension of crystals and compression runs. Unfortunately, this salt did not pass the impurity test – even after several rinses, the surface tension was lower than the literature value and was decreasing too fast. The data are therefore compromised and we do not report them here.

These tests are also useful in view of the wettability problems that are typical for the Wilhelmy plate method. In principle, careful measures need to be taken for the platinum plate

to be wetted completely for the time of the experiment. The completely dry plate requires a significant time to be wetted, due to the large roughness (which assists complete wetting but also makes the wetting process much slower). The established technique that is commonly used in our laboratory to deal with the problem is to wet the plate in advance with pure water for several minutes and dip it in the solution while the plate is still having relatively thick water film. This water film needs some time to drain – for this reason, for the first ~30 s after the plate is dipped, altered σ values are measured. On the other hand, this pure water film makes the wetting significantly faster, especially with salty solutions and monolayers, where the Marangoni effect assists the process.

The presence of a surfactant monolayer is always leading to better wetting, so if there is a wetting problem, it will be worst with the neat water|gas and electrolyte solution|gas surfaces. The fact that we obtain the literature values of the surface tensions of water, 5 mol/kg NaCl and 5 mol/kg NaBr suggest that wetting is complete (the other authors used duNouy ring, maximal pressure in a bubble and other methods that are less susceptible to wetting problems than the Wilhelmy plate technique we are using).

Let us conclude this supplement with a comparison of the adsorptions in Figure 9 (*right*) with those at W|G and W|O at the same salt concentrations (Table S1). The adsorptions Γ_{el0} at the neat interfaces were calculated from the tensiometric data by interpolating them with a polynomial and using the Gibbs equation $\Gamma_{el0} = -d\sigma_0/d\mu_{el}$. In all cases, the adsorption at the LE monolayer is significantly higher than both the W|G and W|O interfaces. This increase is especially pronounced with NaCl.

Table S1. Gibbs adsorption of various electrolytes at various interfaces.

salt	C_m [mol/kg]	Γ_{el0} (W|G) [nm^{-2}]	Γ_{el0} (W|O) [nm^{-2}]	Γ_{el}(W|LE) [nm^{-2}]	tensiometric data from refs
NaF	0.49	–0.10	no data	+0.15÷0.20	71,72
NaCl	0.49	–0.10	–0.10	+0.00÷0.05	1,6,63,72-78
NaCl	2	–0.35	–0.40	+0.45÷0.60	
NaBr	2	–0.35	–0.20	+0.30÷0.45	1,6,72
KCl (octadecanol)	2.13	–0.40	–0.45	+0.00÷0.05 (W|LC, W|S)	1,6,14,26,63, 72,73,76-80

3. EQUILIBRIUM SPREADING TENSION OF $C_{18}H_{37}OH$ CRYSTALS AND CHEMICAL POTENTIAL OF THE MONOLAYER

The spreading tension data[25] we used for the octadecanol are shown in Figure S3. Note that the error bars are slightly different than those in the original work – we could inspect the original data (for which we thank prof. J. Ralston) and found that the uncertainties in ref [25] were overestimated by up to 20%. As discussed in the main text, these uncertainties are important since they control the precision of the final values of the electrolyte adsorption.

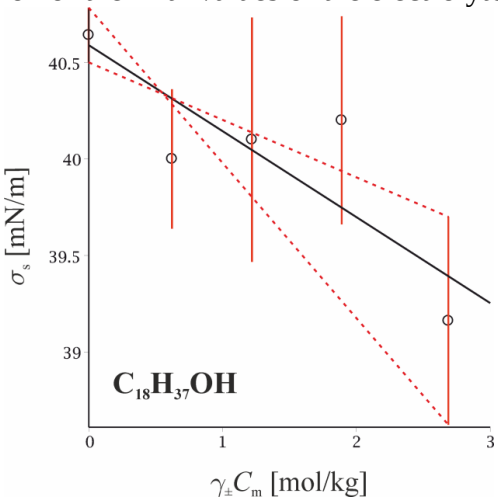

Figure S3. Spreading pressure of $C_{18}H_{37}OH$ crystals onto substrates of various concentrations of KCl (data by Ralston and Healy[25]). The state of the spread monolayer around a pure octadecanol crystal is used as a standard state of the surfactant. From the slope of the linear fit (black line), the values of the adsorption of KCl at the equilibrium spread film follow. The dashed red lines corresponds to linear fit of the σ_s data varied within their uncertainty limits; these are used instead of the black line to estimate the error in the final values of the electrolyte adsorption at any surfactant adsorption.

As a test of the numeric procedure, we calculated $\Delta_s\mu$ by using another procedure, starting from the data for σ vs. Γ^{-1} without the interpolation (9), by approximating the integral (7) to a sum over the experimental data points as described in S4 – eqs S(16)&S(18). The result is illustrated with the points in the inset of Figure S4 and is, within the numerical noise, equivalent to the outcome of the regression.

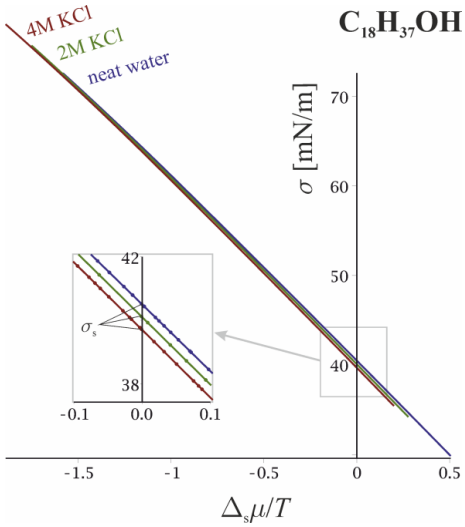

Figure S4. Surface tension σ vs. the chemical potential difference $\Delta_s\mu = \mu - \mu_s$ for octadecanol monolayers at three different KCl concentrations in the substrate. Eq (10) for $\Delta_s\mu(\sigma)$ has been used, as it follows from the surface tension isotherms in Figure 2 and the equilibrium spreading tension of crystals in Figure S3. At a given chemical potential of the surfactant, the surface tension decreases with the increase of the electrolyte concentration (cf. the magnified inset) which corresponds to positive Gibbs adsorption of the salt.

4. CORRECTION OF THE APPARENT AREA PER MOLECULE FOR THE SOLUBILITY OF THE MONOLAYER AND FOR THE KINETIC BARRIER FOR THE LE-LC PHASE TRANSITION

Dodecanol forms monolayers of non-negligible solubility. This leads to a steady decrease of the total adsorbed quantity n. The output of the apparatus is *an apparent adsorption* n_0/A that may be significantly higher than the *actual* adsorption $\Gamma = n/A$ (where n_0 is the initial quantity of surfactant spread on the substrate, A is the area of the monolayer, $n < n_0$ is the actual adsorbed quantity after a fraction of n_0 is dissolved). The driving force of the dissolution process at a given adsorption & surface tension is the difference between the *equilibrium* bulk concentration C_{eq} of the surfactant and the *actual* bulk concentration of the surfactant (which is assumed 0, although non-negligible quantity of surfactant may accumulate in the bulk phase after several runs of the apparatus). The equilibrium concentration C_{eq} follows from the chemical equilibrium condition[81]:

$$\gamma^S \Gamma = K_a C_{eq}, \qquad (1)$$

where K_a is the adsorption constant of the surfactant. From eq S(1) and eqs (2)&(7) it follows that the equilibrium concentration of surfactant C_{eq} is proportional to $\exp(\Delta_s\mu/T)$:

$$C_{eq} = \frac{\gamma_s^S \Gamma_s}{K_a} \exp\left(\frac{\Delta_s \mu}{T}\right), \qquad (2)$$

where γ_s^S is the value of the surface activity coefficient under standard conditions ($\mu_s = \mu_0^S + T\ln\gamma_s^S\Gamma_s$).

To follow the kinetics of the dissolution process, we did several *isobaric runs* for each electrolyte and concentration we studied – these runs are recordings of the surface area A as a function of time t at fixed surface tension σ (Figure S5). In these runs, the monolayers were compressed until a specified surface tension is reached (usually by 5-35 mN/m lower than the surface tension σ_0 of the solution before the monolayer is formed) and then the barostat was switched on. During these experiments, the apparent area per molecule A/n_0 decreases due to the dissolution process, while the real area A/n remains fixed (it is bound to the surface tension according to the equation of state of the monolayer). By measuring the change with time of the surface area at constant surface tension, the solubility of the monolayer was followed and the rate of the process was estimated.

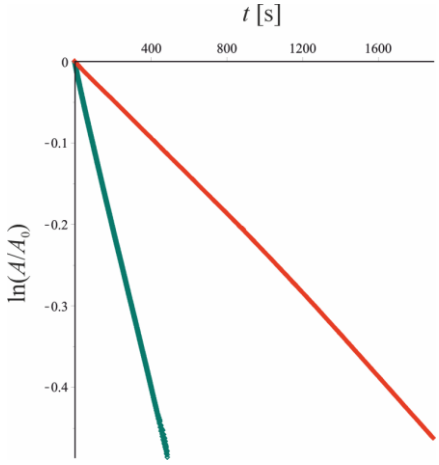

Figure S5. Relative decrease of the area $\ln(A/A_0)$ vs. time t – a run in the isobaric regime at two different compressions of the dodecanol monolayer (red: $\sigma_0 - \sigma = 10$ mN/m; blue: $\sigma_0 - \sigma = 35$ mN/m) at the surface of 5 mol/kg NaCl. A_0 is the initial area. The slope of these lines is used to determine the rate constant controlling the dissolution of the monolayer (k_s in eq S(8)).

Our initial hypothesis was that the process follows diffusion-controlled kinetics, since Defay and Hommelen[82] demonstrated that octanol adsorbs in this regime (although their results for decanol were less conclusive; cf. also the results of Ward and Tordai[83]). We soon found that this was not the case. The solution of Fick's equation for the profile of the surfactant concentration with boundary conditions appropriate for the isobaric regime (time independent adsorption and fixed concentration C_{eq} at the surface; bulk concentration equal to 0) is well-known[84], and the diffusion current of surfactant from the surface to the bulk is given by $j_D = C_{eq}(D/\pi t)^{1/2}$, where D is the diffusion coefficient of the surfactant. The mass balance at the surface reads

$$\frac{1}{A}\frac{\mathrm{d}n}{\mathrm{d}t} = \frac{\Gamma}{A}\frac{\mathrm{d}A}{\mathrm{d}t} = -j_D\,, \tag{3}$$

where we used that Γ is constant in the isobaric regime. Integration of eq S(3) yields $\ln(A/A_0) = -2(C_{eq}/\Gamma)\times(D/\pi)^{1/2}\times t^{1/2}$, where A_0 is the initial area of the monolayer. However, instead of this parabolic dependence on time, we observed a linear one, $\ln(A/A_0) \propto t$, cf. Figure S5. In addition, the process was slower than expected – in the diffusion regime, assuming roughly[83,82] that $D \sim 3\times10^{-10}$ m^2/s and $C_{eq}/\Gamma = \gamma^S/K_a \sim 500$ m^{-1} (this estimate follows from the data of Hommelen[85] and Traube's rule), we find that the ratio A/A_0 will reach 95% after about 10 s; the observed time needed for A/A_0 to reach 95% at neat water surface is longer (~1 min). These findings suggest that the desorption of dodecanol from the dense monolayer is a barrier process. It is also possible that it is a combination of slow barrier desorption and relatively fast *convective* diffusion, since convection is present in the system due to barrier movement, thermal Marangoni (due to evaporation) and Gibbs-Marangoni effects. There are two other processes that result into decrease of n_0: first, it is probable that some leakage of material at the junction of the barrier occurs[54], and second, according to Brooks and Alexander, evaporation of the monolayer[86] can contribute to a certain extent to the loss of material.

Whatever the reason, the linear dependence of the area on time was indicative of dissolution rate proportional to C_{eq}, i.e. instead of eq S(3), the mass balance of the surface should follow the equation

$$\frac{1}{A}\frac{\mathrm{d}n}{\mathrm{d}t} = -kC_{eq}\,, \tag{4}$$

where the *kinetic constant* k is independent of t; this equation is equivalent to *eq 4.31* in ref [87] (at zero bulk concentration of surfactant). We assume that k is also independent on the surfactant activity (in reality, we observed a tendency k to decrease with the increase of Γ, but we neglected it); k depends, however, on the electrolyte concentration. By substituting eq S(2) into eq S(4), we obtain:

$$\frac{1}{A}\frac{\mathrm{d}n}{\mathrm{d}t} = -k_s \exp\left(\frac{\Delta_s\mu}{T}\right), \tag{5}$$

where we introduced a new *adjusted kinetic constant* k_s standing for

$$k_s(C_{el},\sigma_s) = \gamma_s^S\Gamma_s k / K_a(C_{el})\,. \tag{6}$$

Unlike k, the new constant k_s can be determined directly from the isobaric data. For the isobaric regime of the Langmuir balance, where the adsorption Γ is constant, eq S(5) simplifies to:

$$\frac{\Gamma}{A}\frac{\mathrm{d}A}{\mathrm{d}t} = -k_s \exp\left(\frac{\Delta_s\mu}{T}\right). \tag{7}$$

We integrate this *isobaric* equation to obtain:

$$\ln\frac{A}{A_0} = -\frac{k_s}{\Gamma}\exp\left(\frac{\Delta_s\mu}{T}\right)t\,, \tag{8}$$

where A_0 is the initial area (at the start of the isobaric experiment), and A is the area in the moment t. From the slope of the dependence of $\ln(A/A_0)$ vs. t, with known Γ and $\Delta_s\mu$, we obtain k_s. The fact that $\ln(A/A_0)$ vs. t is linear proves the assumption that eq S(4) holds. In some cases we observed deviations from eq S(8) which were indicative of diffusion (dissolution decelerating with time), yet typically the linear law S(8) was valid even after 20-30 min with good accuracy. Actually, often the deviations were positive, i.e. the dissolution was *accelerating* with time. The question for the kinetics of dissolution of the monolayer is interesting and deserves a separate study; for the current work, it is only an auxiliary question and we accept eq S(5) as an empirical fact.

With k_s known, we can proceed to the integration of the kinetic equation S(5) for the normal compression run to obtain the dependence $n(t)$ of the total adsorbed quantity on time:

$$\frac{\mathrm{d}n}{\mathrm{d}t} = -k_s \exp\left(\frac{\Delta_s\mu}{T}\right) A . \tag{9}$$

We divide both sides of this equation by n, and use that $n/A = \Gamma$:

$$\frac{\mathrm{d}n}{n} = -\frac{k_s}{\Gamma} \exp\left(\frac{\Delta_s\mu}{T}\right) \mathrm{d}t . \tag{10}$$

Integration yields:

$$\ln\frac{n}{n_0} = -k_s J , \qquad \text{where } J = \int_0^t \frac{1}{\Gamma} \exp\left(\frac{\Delta_s\mu}{T}\right) \mathrm{d}t . \tag{11}$$

For the solubility correction, the standard state does not have to be fixed to the equilibrium spread monolayer – any convenient state can be chosen, and the symbol σ_s in this section does not necessarily mean "equilibrium spreading tension". If the standard state is chosen as the first measured point of the LE state (subscript 1), one can calculate the values of $\Delta_1\mu(\Gamma_i) \equiv \Delta_1\mu_i$ corresponding to the i-th experimental point using the following iterative formula:

$$\Delta_1\mu_{i+1} = \Delta_1\mu_i + \frac{\sigma_i - \sigma_{i+1}}{2}\left(\frac{1}{\Gamma_{i+1}} + \frac{1}{\Gamma_i}\right); \tag{12}$$

starting from $\Delta_1\mu_1 = 0$, one can calculate all other values $\Delta_1\mu_i$.

Proof of eq S(12). We first convert eq S(7) to a more convenient form by integration by parts:

$$\Delta_s\mu = -\int_{\sigma_s}^{\sigma} \frac{1}{\Gamma}\mathrm{d}\pi = -\int_{\sigma_s}^{\sigma} \mathrm{d}\frac{\sigma}{\Gamma} + \int_{1/\Gamma_s}^{1/\Gamma} \sigma \mathrm{d}\frac{1}{\Gamma} = \frac{\sigma_s}{\Gamma_s} - \frac{\sigma}{\Gamma} + \int_{1/\Gamma_s}^{1/\Gamma} \sigma \mathrm{d}\frac{1}{\Gamma} . \tag{13}$$

Let us assume that the standard state correspond to the first measured point of the LE state. Using the trapezoidal rule, we can discretize the integral as follows:

$$\Delta_1\mu_i = \frac{\sigma_1}{\Gamma_1} - \frac{\sigma_i}{\Gamma_i} + \int_{1/\Gamma_1}^{1/\Gamma_i} \sigma \mathrm{d}\frac{1}{\Gamma} = \frac{\sigma_1}{\Gamma_1} - \frac{\sigma_i}{\Gamma_i} + \sum_{j=1}^{i-1} \int_{1/\Gamma_j}^{1/\Gamma_{j+1}} \sigma \mathrm{d}\frac{1}{\Gamma} , \quad \text{and} \tag{14}$$

$$\int_{1/\Gamma_j}^{1/\Gamma_{j+1}} \sigma \mathrm{d}\frac{1}{\Gamma} = \frac{\sigma_j + \sigma_{j+1}}{2}\left(\frac{1}{\Gamma_{j+1}} - \frac{1}{\Gamma_j}\right). \tag{15}$$

Therefore, $\Delta_1\mu_i$ can be calculated as

$$\Delta_1\mu_i = \frac{\sigma_1}{\Gamma_1} - \frac{\sigma_i}{\Gamma_i} + \sum_{j=1}^{i-1} \frac{\sigma_j + \sigma_{j+1}}{2}\left(\frac{1}{\Gamma_{j+1}} - \frac{1}{\Gamma_j}\right). \tag{16}$$

Here the superscript "1" of Δ means that the first measurement is used as a standard state, and $\Delta_1\mu_i \equiv \Delta_1\mu(\Gamma_i)$. This formula is equivalent to eq S(12).

Let us relate the integrals corresponding to two different standard states, say, those corresponding to the 1st measurement and the equilibrium spread film (s). According to eq S(13),

$$\Delta_1\mu = \frac{\sigma_1}{\Gamma_1} - \frac{\sigma}{\Gamma} + \int_{1/\Gamma_1}^{1/\Gamma} \sigma \mathrm{d}\frac{1}{\Gamma}; \qquad \Delta_s\mu = \frac{\sigma_s}{\Gamma_s} - \frac{\sigma}{\Gamma} - \int_{1/\Gamma_s}^{1/\Gamma} \sigma \mathrm{d}\frac{1}{\Gamma}. \tag{17}$$

These two quantities are related as

$$\Delta_1\mu = \Delta_s\mu + \Delta_1\mu_j, \quad \text{or} \quad \Delta_s\mu = \Delta_1\mu - \Delta_1\mu_s. \tag{18}$$

Here $\Delta_1\mu_s$ is the value of $\Delta_1\mu_i$ with i that corresponds to the value $\sigma_i = \sigma_s$.

We further discretize J, eq S(11), and simplify it:

$$J_i = \sum_{j=1}^{i-1} \int_{t_j}^{t_{j+1}} \frac{1}{T\Gamma} \exp\left(\frac{\Delta_s\mu}{T}\right) \mathrm{d}t = \frac{\Delta t}{2} \sum_{j=1}^{i-1} \left(\frac{\exp\left(\frac{\Delta_s\mu_{j+1}}{T}\right)}{T\Gamma_{j+1}} + \frac{\exp\left(\frac{\Delta_s\mu_j}{T}\right)}{T\Gamma_j} \right) =$$

$$= \Delta t \left(-\frac{\exp\left(\frac{\Delta_s\mu_1}{T}\right)}{2T\Gamma_1} - \frac{\exp\left(\frac{\Delta_s\mu_i}{T}\right)}{2T\Gamma_i} + \sum_{j=1}^{i} \frac{\exp\left(\frac{\Delta_s\mu_j}{T}\right)}{T\Gamma_j} \right). \tag{19}$$

Thus, J can be calculated easily by the recurrent formula:

$$J_{i+1} = J_i + \Delta t \left(\frac{\exp\left(\frac{\Delta_s\mu_i}{T}\right)}{2\Gamma_i} + \frac{\exp\left(\frac{\Delta_s\mu_{i+1}}{T}\right)}{2\Gamma_{i+1}} \right), \tag{20}$$

where $J_1 = 0$. Finally, the corrected adsorption is

$$\Gamma_{\mathrm{corr}} = \frac{n}{n_0}\Gamma_{\mathrm{app}} = \Gamma_{\mathrm{app}} \exp(-k_s J). \tag{21}$$

Since the calculation of k_s through eq S(8) involves $\Delta_s\mu$, which requires the integration of the σ vs. Γ isotherm, the correction procedure is iterative and involves the following steps:

(i) Calculate $\Delta_s\mu$(iter. 1) with eq S(12) using the apparent adsorption of the surfactant Γ_{app};

(ii) Calculate k_s(iter. 1) by application of eq S(8) to the isobaric data (since we use 2-4 isobars, we obtain 2-4 values of k_s; for the following steps, the average is used).

(iii) Calculate the J-integral and the corrected adsorption Γ(iter.1) with eqs S(20)&S(21).

(iv) Repeat (i-iii) using Γ(iter.1) instead of Γ_{app} to obtain Γ(iter.2).

The whole procedure was iterated 1-3 times. In nearly all cases, a single iteration is enough and the second and the third iterations give identical results, within the precision of the experiment. Only for runs of low barrier velocity, where Γ_{corr} was very different from Γ_{app}, a second iteration was needed.

To test the procedure, we made several runs of monolayer compression at 5 mol/kg NaCl, varying the barrier velocity. At the slowest velocity (30 mm/min), the dissolved quantity reached ~50% of n_0, leading to a significant shift of the σ vs. A/n_0 curve at 30 mm/min in comparison with the curve at 200 mm/min, Figure S6 (*left*). After the correction, the data for the LE region become independent of the barrier velocities, Figure S6 (*right*), which proves the usefulness of the procedure. For the highest velocity, the correction leads to actual areas per molecule by 1-2 Å^2 larger than the apparent areas.

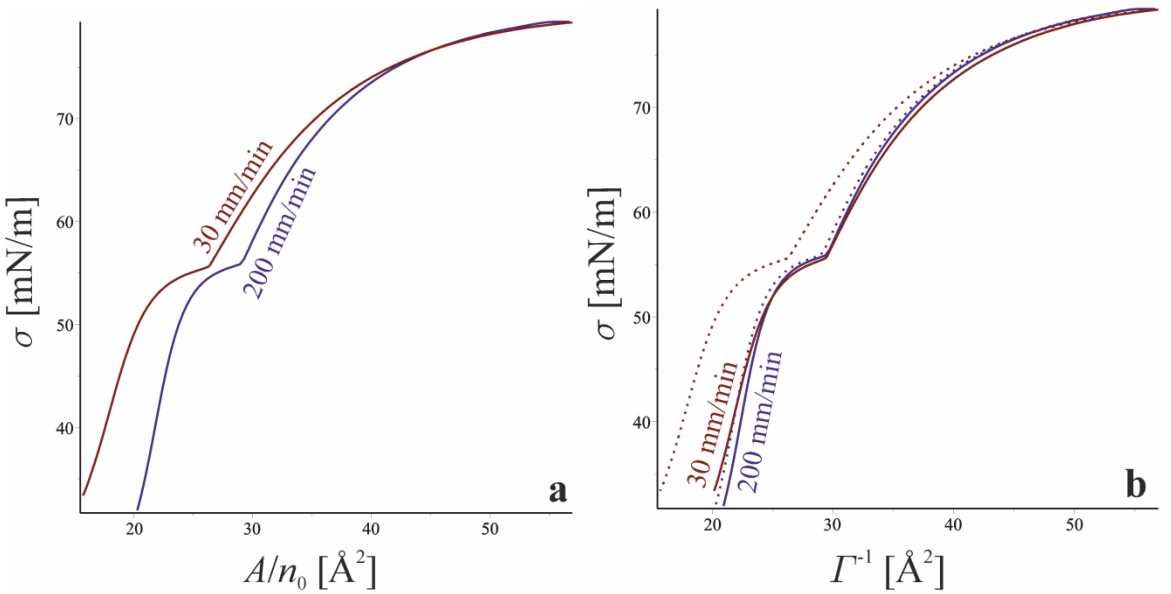

Figure S6. *Left*: surface tension vs. apparent area A/n_0 per molecule of dodecanol spread on a 5 mol/kg aqueous NaCl; data for two different barrier velocities. At the lower velocity, significant amount of the surfactant dissolves so that the actual quantity at the surface is $n << n_0$, and therefore the shift towards smaller areas. *Right*: the same data after the correction for the dissolved quantity of surfactant – the two runs compare well to each other, within the precision of the experiment.

Another test of our data after the correction is the comparison of our isotherms for dodecanol at 21.0 and 26.3°C (no salt) with those of Fainerman et al.[46] at 10 and 15°C, shown in Figure S7 (*left*). The four curves are showing a smooth trend after the solubility correction.

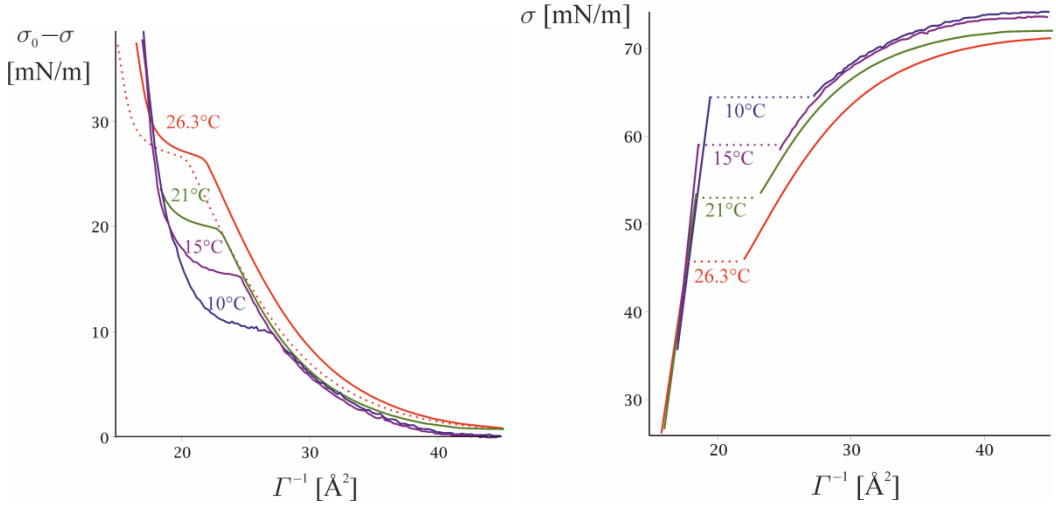

Figure S7. *Left*: comparison of our surface pressure $\sigma_0 - \sigma$ vs. area Γ^{-1} isotherms (dodecanol, no salt, 21 and 26.3°C) with the data of Fainerman et al.[46] (10 and 15°C). The dashed line is the data at 26.3°C before the correction for the solubility. *Right*: the same data after the correction for the kinetic effects during the LE-LC phase transition.

The next problem we had to deal with was the kinetic effects during the phase transition LC-LE. The main problem in this region is that once the LC domains are formed, they start to interact repulsively with each other[55], and the force applied by the barrier on the heterogeneous monolayer is partly acting against this repulsive force (similar effects are common in the three dimensional liquid-solid phase transitions, when the fractal net of solid crystals in touch with each other start to have an elastic answer against the external force). There are several additional reasons the data in the LC zone to be far from exact. The first is that the kinetic constant k in the LC zone must be different from the one in the LE phase, while we applied eq (4) to the data for both, which is clearly an approximation. In addition, we observed an apparent decrease of the monolayer compressibility near the point of collapse, which is physically unrealistic; this

might be an indication for the formation of three-dimensional structures at tension higher than σ_s (at which the first 3D crystals should occur). In view of these complications, we decided that the crudest approximation for the equilibrium shape of the LC region – a line – is good enough. The following procedure was applied to all data:

(i) Identify the point at which the phase transition starts (indicated with an arrow in Figure S7); the data right of this point corresponds to homogeneous LE phase, while the data left of it refers to a heterogeneous surface with LC domains dispersed in an LE film (probably, the system relaxes to homogeneous LC monolayer eventually, but it is very likely that the LC domains and the two-dimensional LE films between them will survive even at very significant compressions, close to the collapse).

(ii) The data in the LE region is fitted with eq (16) ($\sigma > \sigma_t$) – let the respective function be $f^{LE}(\sigma)$. The data for the heterogeneous monolayer is fitted with a polynomial (of degree 3 or 4); we call the respective function $f^{het}(\sigma)$.

(iii) The point at which $f^{LE}(\sigma) = f^{het}(\sigma)$ identifies the phase transition tension σ_t and the respective equilibrium LE adsorption Γ^{LE}.

(iv) The data for the heterogeneous monolayer has an inflection. The tangent line through the inflection point of f^{het} is constructed and is assumed to represent the equilibrium state of the LC monolayer (the equilibrium LC line in Figure S8).

(v) The point of cross-section of the equilibrium LC line and the horizontal line $\sigma = \sigma_t$ defines the area of the LC monolayer in equilibrium with the LE film.

(vi) The value of the equilibrium spreading pressure σ_t is substituted in the equation for the equilibrium LC line; this yields the area of the equilibrium spread layer.

This procedure is illustrated in detail in Figure S8. It is also illustrated with the data for pure water substrates in Figure S7: the left figure is before the LC-LE correction, and the right one is after it. The edges of the horizontal dashed lines are part of the binodal for the LE-LC transition. It is remarkable that the slope of the LC region in Figure S7 (*right*) does not depend on the temperature significantly (both for our data and the data of Fainerman et al.[46]).

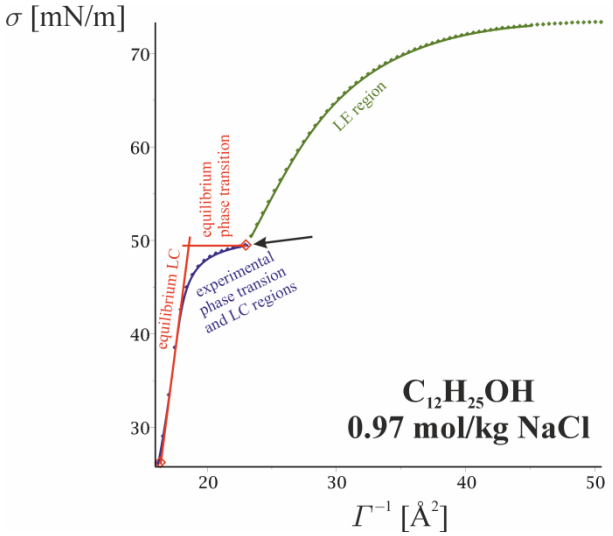

Figure S8. Correction for the kinetic effects during the LC-LE phase transition. The significant repulsion between the LC domains formed during the phase transition leads to kinetic increase surface pressure $\sigma_0 - \sigma$. The observed σ vs. Γ^{-1} curve in this region is therefore below the theoretically expected horizontal line for a first order phase transition.

A third, relatively small correction was made for the temperature difference between the measurements – we reduced all data to the average temperature of all runs for the same electrolyte, assuming surface entropy of 0.138 mN/Km.

We usually did 4-5 runs on the same substrate. In relation to that, another problem we met is that due to the dissolution process, surfactant accumulation in the substrate occurs. In each next run, we would rinse the surface until the initial surface tension is reached. Nevertheless, in each next run slower dissolution was evident (isotherms shift towards larger apparent areas), which means that the bulk concentration of the surfactant increases noticeably. The dissolution of the surfactant in the substrate and its subsequent adsorption at the reference electrode may cause also biased ΔV-potential measurements. We tried to minimize the error stemming from this problem by (i) using data from the first 2-3 runs only; (ii) by doing the runs with higher barrier velocity before the slower runs (the latter contaminate the substrate far more significantly); (iii) by neglecting the data for the largest areas per molecule, which were affected by the accumulation to a larger extent.

5. PARAMETERS OF THE REGRESSION OF THE σ VS. Γ DATA

The regression approach is widely used in physics to rationalize the data for activity, dielectric constant, equation of state etc. (e.g., ref [41]). We found it reasonable to rationalize the data we use for the surface tension vs. surfactant area as well, by fitting them with the stepwise functions (9)&(16). In the case of octadecanol, the "data points" we fit are the digitalized figures from ref [25]; the use of eq (9) is neither taking away nor adding any significant information to these points. In the case of dodecanol, the lines (16) differ from the original values in the LE region within their precision limit. In the LC phase and in the phase transition regions, when correcting for the kinetic effects during phase transition (cf. S4), we approximate the σ vs. Γ^{-1} data with lines anyway. The parameters of the regression functions are listed in Table S2, Table S3 & Table S4.

The limits in which the regressions are valid are given as well. In the case of octadecanol, the monolayer can be compressed to metastable state where $\sigma < \sigma_s$, probably due to the barrier for nucleation. For this reason, the minimal experimental value in Table S2 is smaller than σ_s. In the case of dodecanol, the collapse occurs close to $\sigma = \sigma_s$.

The parameter values in the following tables should be used with the given accuracy, otherwise significant rounding errors occur.

Table S2. Regression of the data of Ralston and Healy[25] for the area vs. surface tension with eq (9).

	neat water	**2M KCl**	**4M KCl**
Γ_t^{-1} [Å^2]	19.83	19.80	19.78
σ_t [mN/m]	60.18	61.65	63.13
g_1^{LC} [m^3/N] $\times 10^{20}$	116.58	125.37	156.61
g_2^{LC} [m^4/N^2] $\times 10^{20}$	7069.0	-3578.5	-3833.8
g_3^{LC} [m^5/N^3] $\times 10^{20}$	-1.3545×10^6	3.3309×10^5	2.7158×10^5
g_4^{LC} [m^6/N^4] $\times 10^{20}$	7.7683×10^7	0	0
g_1^{S} [m^3/N] $\times 10^{20}$	23.768	29.197	31.351
g_2^{S} [m^4/N^2] $\times 10^{20}$	80.853	61.269	68.436
g_3^{S} [m^5/N^3] $\times 10^{20}$	1293.1	0	0
g_4^{S} [m^6/N^4] $\times 10^{20}$	0	0	0
σ_{max} [mN/m]	72.6	75.7	78.1
σ_{min} [mN/m]	29.8	34.2	35.4

Table S3. Dodecanol spread on water and NaCl solutions – data summary, eq (16).

	neat water	neat water	0.49 mol/kg NaCl	0.97 mol/kg NaCl	2.0 mol/kg NaCl	2.0 mol/kg NaCl	5.0 mol/kg NaCl
T [°C]	21.0	26.3	25.6	25.2	22.5	23.9	23.4
σ_{max} [mN/m]	72.0	70.9	72.0	73.0	75.2	73.5	78.9
σ_t [mN/m]	53.000	45.514	47.502	49.439	52.099	51.352	54.821
g_1^{LE} [Å^2]	0.28162	0.091152	0.25697	0.22126	2.2766	1.9896	0.92644
g_0^{LE} [N/m]	-13.17065	-15.26471	-5.443234	-7.20708	-1.33371	-1.428256	-2.13933
g_{-1}^{LE} [N^2/m^2]	-1.273396	-1.169032	-0.4071500	-0.594110	-0.130018	-0.1503176	-0.209776
g_{-2}^{LE} [N^3/m^3]	0.01778233	0.01361663	0.004747518	0.00731518	0.00182666	0.002159087	0.00284624
g_{ln}^{LE} [N/m]	-10.39505	-10.94739	-3.842561	-5.31021	-1.02886	-1.145950	-1.67669
g_{d0}^{LE} [N/m]	-0.03795767	-0.02696029	-0.02708925	-0.0288282	-0.0413048	-0.04204222	-0.0343888
g_{d2}^{LE} [m/N]	-6.572076	-12.21000	-12.16512	-11.3357	-6.01051	-5.892407	-9.29938
g_{d3}^{LE} [m^2/N^2]	0	48.91879	48.63318	41.7179	0	0	27.1082
g_0^{LC} [Å^2]	13.596	13.178	13.460	13.960	11.961	13.601	12.270
g_1^{LC} [Å^{2}m/N]	88.893	98.537	88.141	93.363	191.23	157.42	231.95

Table S4. Dodecanol spread on NaF and NaBr solutions – data summary, eq (16).

	0.49 mol/kg NaF	0.97 mol/kg NaF	2.0 mol/kg NaBr	5.0 mol/kg NaBr
T [°C]	25.6	24.8	18.5	19.8
σ_{max} [mN/m]	72.4	73.3	75.9	78.0
σ_t [mN/m]	48.593	49.852	54.198	54.060
g_1^{LE} [Å^2]	0.61574	0.45257	0.12482	-22494
g_0^{LE} [N/m]	-4.13263	-6.53372	-14.79251	3.124805
g_{-1}^{LE} [N^2/m^2]	-0.417387	-0.669515	-1.308734	0.5472593
g_{-2}^{LE} [N^3/m^3]	0.00568729	0.00923041	0.01654293	-0.01483615
g_{-3}^{LE} [N^4/m^4]	0	0	0	0.0001779907
g_{ln}^{LE} [N/m]	-3.32742	-5.30815	-11.28060	3.206354
g_{d0}^{LE} [N/m]	-0.0390850	-0.0392716	-0.02977287	-61.01871
g_{d2}^{LE} [m/N]	-6.36568	-6.34195	-10.97918	44030.72
g_{d3}^{LE} [m^2/N^2]	0	0	39.14486	-415456.4
g_0^{LC} [Å^2]	13.298	14.231	12.688	9.8600
g_1^{LC} [Å^{2}m/N]	100.42	115.96	184.19	302.82

6. THE REVERSE THERMODYNAMIC PROBLEM

Here we consider the thermodynamic problem opposite to the one discussed in the *Theoretical basis* section. Let the dependences $\Gamma_{el}(\Gamma, C_m)$ and $\sigma(\Gamma, C_m = 0)$ be known. Find $\sigma(\Gamma, C_m)$. From the Gibbs isotherm (1), two differential equations for $\sigma(\Gamma, C_m)$ and $\mu(\Gamma, C_m)$ follow:

$$\left(\frac{\partial\sigma}{\partial C_m}\right)_\Gamma = -2\Gamma_{el}\frac{d\mu_{el}}{dC_m} - \Gamma\left(\frac{\partial\mu}{\partial C_m}\right)_\Gamma \quad \text{and}$$

$$\left(\frac{\partial\sigma}{\partial\Gamma}\right)_{C_m} = -\Gamma\left(\frac{\partial\mu}{\partial\Gamma}\right)_{C_m}. \qquad (22)$$

Their general solution reads

$$\mu(\Gamma, C_m) = \mu(\Gamma, C_m = 0) - 2\int_0^{C_m}\frac{\partial\Gamma_{el}(\Gamma, C_m)}{\partial\Gamma}\frac{d\mu_{el}}{dC_m}dC_m \quad \text{and}$$

$$\sigma(\Gamma, C_m) = \sigma_0 - \int_0^{\Gamma}\Gamma\frac{d\mu(\Gamma, C_m = 0)}{d\Gamma}d\Gamma + 2\Gamma^2\int_0^{C_m}\frac{\partial\Gamma_{el}(\Gamma, C_m)/\Gamma}{\partial\Gamma}\frac{d\mu_{el}}{dC_m}dC_m, \qquad (23)$$

where $\mu(\Gamma, C_m = 0)$ (surfactant's chemical potential on neat water) is still unknown. Setting $C_m = 0$ in the right hand side of eq S(23), and using that the result is equal to the known function $\sigma(\Gamma, C_m = 0)$ (i.e. we apply a boundary condition), we eliminate the unknown $\mu(\Gamma, C_m = 0)$:

$$\sigma(\Gamma, C_m) = \sigma(\Gamma, C_m = 0) + 2T\Gamma^2\int_0^{C_m}\frac{\partial\Gamma_{el}(\Gamma, C_m)/\Gamma}{\partial\Gamma}\frac{d\ln\gamma_{\pm}C_m}{dC_m}dC_m. \qquad (24)$$

From this equation it becomes obvious why $\sigma(\Gamma, C_m)$ is not enough to determine $\Gamma_{el}(\Gamma, C_m)$. All functions $\Gamma_{el}(\Gamma, C_m)$ for which the derivative $\partial(\Gamma_{el}(\Gamma, C_m)/\Gamma)/\partial\Gamma$ is the same lead to the same $\sigma(\Gamma, C_m)$, which means that if $\sigma(\Gamma, C_m)$ is known, $\Gamma_{el}(\Gamma, C_m)$ can be determined with accuracy up to a term $k\Gamma$, where k is an arbitrary constant (that may depend on C_m).

Let us give a simple example of how eq S(24) can be used in practice. Let us assume that the following equation of state holds for the electrolyte adsorption:

$$\Gamma_{el}(\Gamma, C_m) = K(\Gamma)C_m; \qquad (25)$$

here K is the adsorption constant of the electrolyte, which is a function of the surfactant adsorption Γ. Eq (25) is in qualitative agreement with the data in Figure 3 & Figure 7. The substitution of eq S(25) in eq S(24) leads to the following formula for σ:

$$\sigma(\Gamma, C_m) = \sigma(\Gamma, C_m = 0) + 2T\Gamma^2\frac{\partial K(\Gamma)/\Gamma}{\partial\Gamma}\gamma_w C_m. \qquad (26)$$

Thus, if the dependence of K on Γ could be determined theoretically, the effect of the salt on the σ vs. Γ isotherm follows immediately.

7. KINETICS OF SPREADING OF THE MONOLAYER AROUND DODECANOL CRYSTALS

The measurements were performed with a platinum plate and an analytic balance (Sartorius 211D) in a small Teflon trough equipped with two Teflon barriers. Before each measurement, the surface is rinsed with the first Teflon barrier, which passes from the one end of the trough to the other, and remains there. The second barrier is then put in the middle of the trough, thus dividing the surface into two compartments. The platinum plate is dipped in the first *plate compartment*; the dodecanol crystals are dispersed in the second. The dodecanol is a paste made of fine crystals that are visible upon spreading at the surface. At the higher temperatures, the crystals melt once they attach to the surface which did not cause any observable problems with the measurement. The second barrier is then removed, which is considered to be the beginning of the experiment (t = 0). This procedure was developed in order to avoid the attachment of $C_{12}H_{25}OH$ crystals or drops to the meniscus of the plate, which affects the measured weight of the meniscus[25]. With this experimental design, the dodecanol crystals remain at the meniscus of the trough, far away from the Pt plate.

As a rule, the data for highly concentrated solutions were of better reproducibility than the data for pure water and solutions of lower concentration.

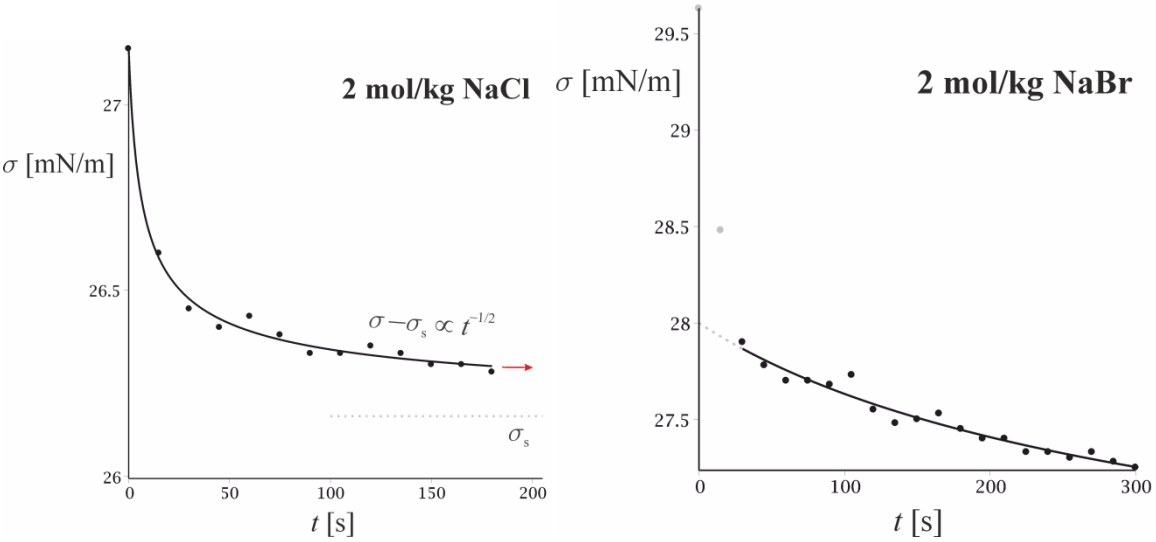

Figure S9. Time-dependant spreading tension of dodecanol crystals. Lines are fits with eq (27).

The typical kinetics of spreading of the monolayer around the crystal is illustrated in Figure S9 (*left*). Slow diffusion kinetics was evident in all cases; therefore, to extrapolate to equilibrium, the data were fitted with a $t^{-1/2}$ law:

$$\sigma(t) = \sigma_s + a / \sqrt{t_0 + t}\,, \qquad (27)$$

cf. the line in Figure S9 (*left*).

The difference between the initial $\sigma(t = 0)$ and the limit σ_s at $t \to \infty$ was typically less or around 2 mN/m, i.e. the initial state was close to equilibrium. The only exception was the 2 mol/kg NaBr substrate, which was not well saturated, perhaps due to a temperature jump between the saturation period and the measurement. In result, the equilibration was much slower. Nevertheless, the extrapolated values for σ_s for the 3 runs we made were in good agreement so we did not repeat the experiment.

In the first 30-60 s of several measurements, we observed more complicated kinetics than the square root law (27) (e.g., initial positive slope of σ vs. t, with a maximal value). In these cases, the initial kinetics was neglected.

8. CONCENTRATION AND HOFMEISTER EFFECTS ON DODECANOL MONOLAYERS: ADDITIONAL FIGURES

In Figure S10 we present the surface pressure $\sigma_0 - \sigma$ vs. area Γ^{-1} per dodecanol molecule at various concentrations and electrolytes. The observed increase of $\sigma_0 - \sigma$ with the increase of the concentration C_m of NaCl (*left*) and with the change of the anion to Br^- at fixed C_m (*right*) means increase of the lateral repulsion (or decrease of the lateral attraction) in the monolayer. This can be due to a combination of charging of the monolayer by the adsorbed ion and to the electrolyte screening of the lateral van der Waals attraction between the dodecanol molecules in the monolayer (compare to the findings of Petrache at al.[36,61]). The trends we observe are similar to those found in other studies of non-ionic monolayers[32,88,89]. Note, however, that the $\sigma_0 - \sigma$ trends are not directly related to those for Γ_{el}, cf. the *Theoretical basis* section.

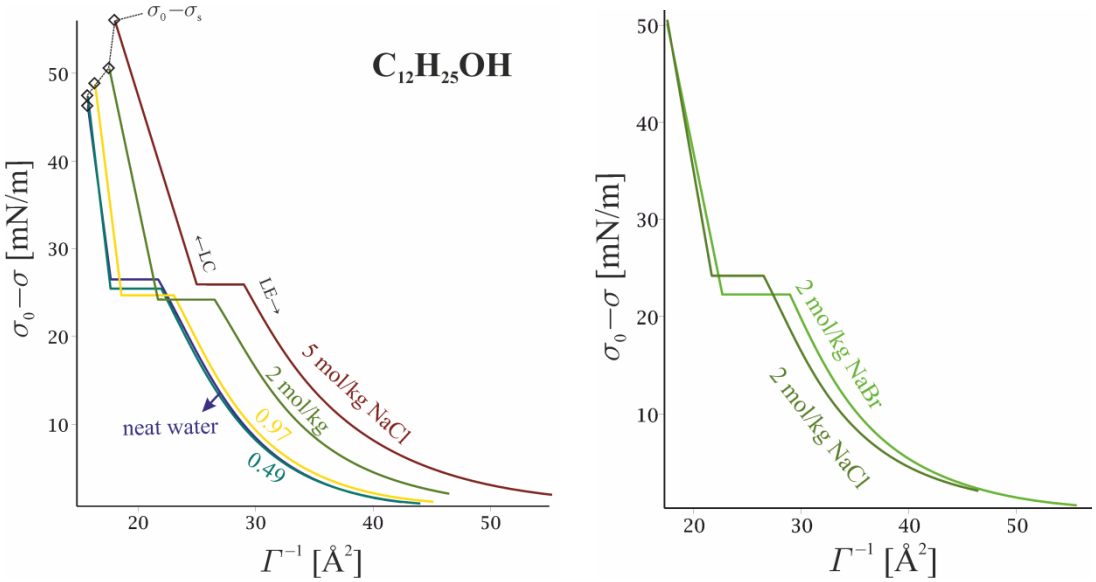

Figure S10. Surface pressure $\sigma_0 - \sigma$ as a function of the area per dodecanol molecule for NaCl substrates at various concentrations (*left*) and for NaCl and NaBr at the same concentration (*right*).

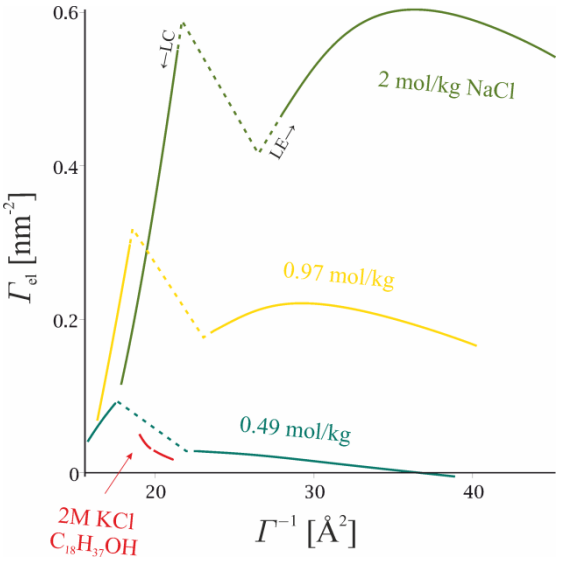

Figure S11. NaCl's Gibbs adsorption Γ_{el} as a function of area per surfactant molecule Γ^{-1}. This is a parametric plot of $\Gamma_{el}(\sigma)$ against $\Gamma^{-1}(\sigma)$. The data for octadecanol over aqueous KCl from Figure 3 is shown for comparison.

The adsorption of NaCl at a dodecanol monolayer as function of the area per surfactant molecule is given in Figure S11. The adsorption of KCl at an octadecanol monolayer is also plotted for comparison. The ε-discontinuity adsorption $\Gamma_{el}^{z=0}$ of NaCl is given as a function of the area per dodecanol molecule in Figure S12. In comparison with the Gibbs adsorption Γ_{el} in Figure 7, $\Gamma_{el}^{z=0}$ is significantly lower. In the case of 0.49 mol/kg NaCl, it is even negative (NaCl is repulsed by the surface of discontinuity of the dielectric permittivity at this concentration).

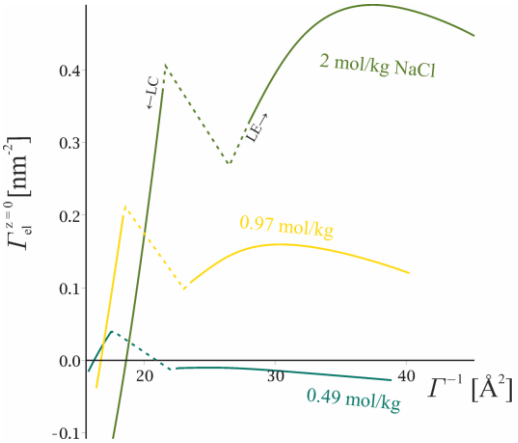

Figure S12. The adsorption $\Gamma_{el}^{z=0}$ of NaCl at the surface of discontinuity of the dielectric permittivity as a function of the area per surfactant molecule $1/\Gamma$. The adsorption $\Gamma_{el}^{z=0}$ follows from eq (14) and the data in Figure 7.

9. COMPARISON OF THE EXPERIMENTAL POTENTIAL ϕ^{DL} OF THE ELECTRIC DOUBLE LAYER AND THE ELECTROLYTE ADSORPTION WITHIN GOUY'S MODEL

Let the ions of a 1:1 electrolyte be specifically adsorbed at a surface (with adsorptions Γ_+^A and Γ_-^A in the adsorption layer). These adsorptions result into a surface charge $e(\Gamma_+^A - \Gamma_-^A)$, and the formation of a *diffuse* layer, in which the adsorptions of the two ions are Γ_+^D and Γ_-^D. The distribution of ions results also in a double layer potential ϕ^{DL}. Gouy's model predicts several relations between the above quantities – first, Gouy's equation:

$$\Gamma_+^A - \Gamma_-^A = 2C_{el}L_D\left(\Phi^{-1/2} - \Phi^{1/2}\right). \tag{28}$$

Here,

$$\Phi = \exp(-e\phi^{DL}/T) \tag{29}$$

is the surface Boltzmann factor and L_D is the Debye length, defined with

$$L_D^2 = \varepsilon^W T / 2e^2 C_{el}.$$

A second consequence of Gouy's model stems from the integration of the concentration profiles in the diffuse layer, which leads to a relation between the diffuse layer adsorptions and the surface potential:

$$\Gamma_+^D = 2C_{el}L_D\left(\Phi^{1/2} - 1\right) \quad \text{and} \quad \Gamma_-^D = 2C_{el}L_D\left(\Phi^{-1/2} - 1\right). \tag{30}$$

According to the results from Figure 10, the cation dominates the adsorption layer. We can therefore assume that

$$\Gamma_-^A \approx 0. \tag{31}$$

The total electrolyte adsorption in this case is:

$$\Gamma_{el} = \Gamma_-^D = \Gamma_+^A + \Gamma_+^D = 2C_{el}L_D\left(\Phi^{-1/2} - 1\right). \tag{32}$$

Eqs S(29)&S(32) allow ϕ^{DL} to be calculated from the Gibbs adsorption of NaCl in Figure 9 (*right*). The result is shown in Figure 10 (*right*) – dashed line. The potential that follows from Gouy's theory is by about 20 mV higher than the one that follows from the Volta potential. The difference is most probably due to the approximate nature of eqs (22),S(31)&S(32). One very natural explanation is that there is a non-zero specific adsorption of the anion, but this cannot be claimed based solely on the data Figure 10 (*right*).

10. ADDITIONAL REFERENCES

71. Matubayasi, N.; Tsunetomo, K.; Sato, I.; Akizuki, R.; Morishita, T.; Matuzawa, A.; Natsukari, Y. Thermodynamic quantities of surface formation of aqueous electrolyte solutions IV. Sodium halides, anion mixtures, and sea water. *J. Colloid Interface Sci.* **2001**, *243*, 444-456.
72. Weissenborn, P.K.; Pugh, R.J. Surface tension of aqueous solutions of electrolytes: relationship with ion hydration, oxygen solubility, and bubble coalescence. *J. Colloid Interface Sci.* **1996**, *184*, 550-563.
73. Abramzon, A.A.; Gaukhberg, R.D. Surface tension of salt solutions. *Russ. J. Appl. Chem.* **1993**, *66*, 1896; 1665.

74. Ozdemir, O.; Karakashev, S.I.; Nguyen, A.V.; Miller, J.D. Adsorption and surface tension analysis of concentrated alkali halide brine solutions. *Minerals Eng.* **2009**, *22*, 263-271.
75. Pegram, L.M.; Record, M.T. Hofmeister salt effects on surface tension arise from partitioning of anions and cations between bulk water and the air-water interface. *J. Phys. Chem. B* **2007**, *111*, 5411-5417.
76. Kidokoro, M. The interfacial tensions between hexane and aqueous salt solutions. *Bull. Chem. Soc. Jpn.* **1932**, *8*, 280-286.
77. Evans, A.W. The effect of uni-univalent electrolytes upon the interfacial tension between normal-hexane and water. *Trans. Faraday Soc.* **1937**, *33*, 794-800.
78. Guest, W.L.; Lewis, W.C.M. The effect of electrolytes upon the interfacial tension between water and dekalin (trans-decahydronaphthalene). *Proc. R. Soc. A* **1939**, *170*, 501-513.
79. Martens, L.K., ed. *Technical encyclopedia*, Vol 10. OGIZ, Moscow, 1933 (in Russian).
80. Lide, D. R., ed. *CRC Handbook of chemistry and physics*, 77th ed. CRC Press, New York, 1996.
81. Slavchov, R.I.; Dimitrova, I.M.; Ivanov, I.B. Cohesive and non-cohesive adsorption of surfactants at liquid interfaces. In: Rubio, R.G.; Ryazantsev, Y.S.; Starov, V.M.; Huang, G.X.; Chetverikov, A.P.; Arena, P.; Nepomnyashchy, A.A.; Ferrús, A.; Morozov, E.G., eds. *Without bounds: a scientific canvas of nonlinearity and complex dynamics*. Springer-Verlag, 2013.
82. Defay, R.; Hommelen, J.R. The importance of diffusion in the adsorption process of some alcohols and acids in dilute aqueous solutions. *J. Colloid Sci.* **1959**, *14*, 411–418.
83. Ward, A.F.H.; Tordai, L. Time-dependence of boundary tensions of solutions I. *J. Chem. Phys.* **1946**, *14*, 453–461.
84. Crank, J. *The mathematics of diffusion*, 2nd ed. Clarendon Press, Oxford, 1975, sec. 2.4.2.
85. Hommelen, J.R. The elimination of errors due to evaporation of the solute in the determination of surface tensions. *J. Colloid Sci.* **1959**, *14*, 385–400.
86. Brooks, J.H.; Alexander, A.E. Spreading and collapse phenomena in fatty alcohol series. *J. Phys. Chem.* **1962**, *66*, 1851–1853.
87. Dukhin, S.S.; Kretzschmar, G.; Miller, R. *Dynamics of adsorption at liquid interfaces, theory, experiment, application*. Elsevier, 1995, sec. 4.4.
88. Viswanath, P.; Aroti, A.; Motschmann, H.; Leontidis, E. Vibrational sum frequency generation spectroscopic investigation of the interaction of thiocyanate ions with zwitterionic phospholipid monolayers at the air−water interface. *J. Phys. Chem. B* **2009**, *113*, 14816–14823.
89. Leontidis, E.; Aroti, A.; Belloni, L. Liquid expanded monolayers of lipids as model systems to understand the anionic Hofmeister series 1. *J. Phys. Chem. B* **2009**, *113*, 1447–1459.